Journal of the Indian Chemical Society 99 (2022) 100318

Contents lists available at ScienceDirect

Journal of the Indian Chemical Society

journal homepage: www.editorialmanager.com/JINCS/default.aspx

Ultrasound-assisted adsorption of Pb ions by carbonized/activated date stones from singles/mixed aqueous solutions

Nora Sedira [a], Saliha Bouranene [b,*], Abdalhak Gheid [a,c]

[a] Department of Material Sciences, Faculty of Sciences and Technology, University of Mohamed Cherif Messaadia, BP 1553, 41000, Souk-Ahras, Algeria
[b] Department of Process Engineering, Faculty of Sciences and Technology, University of Mohamed Cherif Messaadia, BP 1553, 41000, Souk-Ahras, Algeria
[c] Laboratory of Science and Technology of Water and Environment LST2E, Mohammed Cherif Messaadia University, BP 1553, 41000, Souk-Ahras, Algeria

ARTICLE INFO

Keywords:
Adsorption
Date stones
Carbonization
Activation
Lead ions
Mixed solutions
Ultrasound

ABSTRACT

This work aims to assess the adsorption efficiency of date stones biowaste subjected to carbonization and activation processes for the removal of Pb ions from single and mixed solutions. Several techniques have been used for characterization of adsorbents such as scanning electron microscopy (SEM), Fourier transform infrared spectroscopy (FTIR), methylene blue index and point of zero charge (pHpzc). An excellent adsorption capacity of 97.43% is achieved at an initial concentration of 300 mg/L, solution volume 75 mL of Pb nitrate, adsorbent mass of 0.7 g, temperature of 30 °C, a stirring speed of 500 rpm/min, a contact time of 180 min and pH 6. Specifically, a comparison has been conducted between carbonized/activated date stones "CADS" and commercial activated carbon "CAC" besides investigating the influence of the presence of Co ions and the utilization of ultrasound radiation. A higher adsorption rate of 98.16% is reached under ultrasound radiation at Pb(II) initial concentration of 100 mg/L for a contact time of 3 h. Nevertheless, the temperature has shown a negative effect; the adsorption rate decreases from 98.31% at 18 °C to 92.70% at 60 °C. The modeling of the experimental adsorption data manifests a type-L isotherm characteristic of Langmuir and Freundlich models. The kinetic study has shown that the experimental data are well described by a pseudo-second-order rate model and controlled by the internal diffusion, a limiting-step that controls the transfer rate of Pb(II) to the adsorbent surface. The calculated thermodynamic parameters (ΔG^0, ΔH^0, ΔS^0) indicate that the adsorption of Pb(II) is spontaneous and exothermic process.

1. Introduction

Heavy metals are in fact highly toxic species beyond a certain concentration. They have the ability to concentrate along the food chain and accumulate in certain body organs. It is therefore necessary to eliminate completely heavy metal ions present in different industrial effluents or reduce their amount below the limits defined by standards [1]. Lead (Pb) present in various industrial effluents, constitutes a large part of the water pollution and exposure to this contaminant, even at low concentrations may be harmful to human health because of its impact on the development of serious diseases and disorders. The removal of Pb ions from industrial and municipal wastewaters has become of extreme importance and extensive efforts have been devoted to the development of effective methods for the removal of these ions from wastewaters [2].

Many decontamination methods are developed in recent years, including chemical precipitation, flocculation, ion exchange, electrolysis, and membrane processes [3]. In this regard, the adsorption of heavy metals onto solids has attracted great attention and has been widely investigated.

Among the materials widely utilized during this process are activated carbon prepared from biomaterials such as olive pits which has removed 72% of mercury (II) cations for a mass of 0.5 g of adsorbent, and also activated carbon prepared from bicarbonate treated peanut hulls carbons which was found to be more effective in the treatment of mercury solutions by giving an adsorption efficiency of 109.89 mg/g in comparison to commercial activated carbon which has shown an adsorption efficiency of 12.38 mg/g [4].

Fronczak et al. showed that the functionalization of the activated carbon grains with cysteine and thiourea greatly improved the adsorption capacity of Cd (II) compared to activated carbon [5]. The removal of heavy metals by adsorption process has been also investigated using various metal oxides, namely oxides of iron, titanium, manganese,

* Corresponding author.,
E-mail addresses: saliha.bouranene@univ-soukahras.dz, saliha.bouranene@yahoo.fr (S. Bouranene).

https://doi.org/10.1016/j.jics.2021.100318
Received 16 October 2021; Received in revised form 4 December 2021; Accepted 16 December 2021

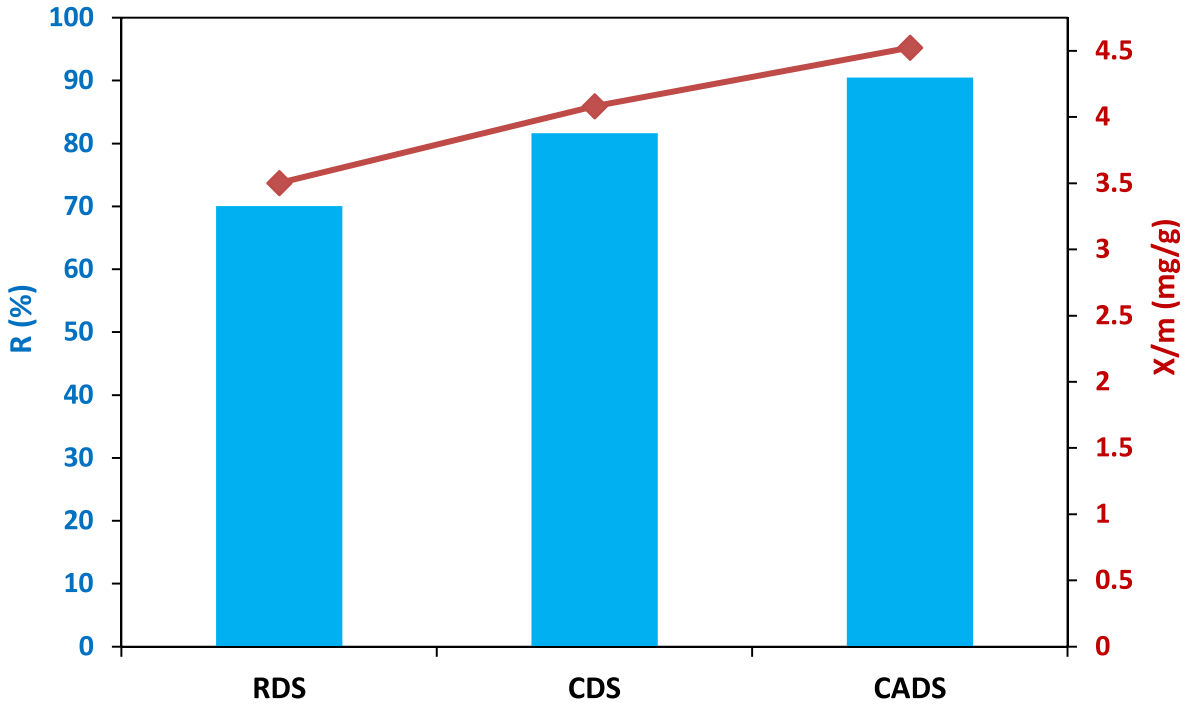

Fig. 1. Adsorption rate of Pb ions as function of adsorbent nature (RDS, CDS and CADS). $[Pb^{2}+]_0$ = 100 mg/L; adsorbent mass = 0.5g; $V_{soluion}$ = 25 mL; stirring speed = 500 rpm; contact time = 6 h; pH = 5.6 ± 0.2; T = 18 ± 2 °C.

magnesium, aluminum, etc. The study of the influence of some parameters affecting the adsorption efficiency such as porosity, temperature and morphology was examined [6]. On the other hand, the development of metal-organic framework added to graphene-based two-dimensional and three-dimensional materials, allowed researchers to recover metal ions with good adsorption efficiency [7].

Some authors have studied the adsorption of heavy metals on calcium nanotitanate under different operational conditions in terms of pH, temperature and concentration. The high adsorption capacities of Pb, Cd and Zn on perovskite were 141.8, 18.0 and 24.4 mg/g, respectively [8].

Liu et al. have developed a bio-adsorbent based on the immobilization of caffeic acid on corn starch ialdehyde. The adsorbent has proven effective in treating hexavalent chromium pollution due to its easy synthesis, ultra-high selectivity and excellent adsorption performance. The maximum amount of Cr (VI) removal was 96.45 mg/g. The adsorption kinetics and isotherm indicated that the adsorption of Cr (VI) onto adsorbent was controlled by a heterogeneous chemisorption process [9].

Clays, as natural and abundant low-cost materials, represent another type of solid adsorbents [10–13]. Both montmorillonite and kaolin were identified as good adsorbents of Pb ions in aqueous media. It was found that increasing the pH promotes the removal of metal ions until the appearance of insoluble precipitates (i.e. presence of hydroxides). The absorption was rapid between 180 min and 240 min. Several isotherm models were adopted to evaluate the adsorption equilibrium, kinetics and mechanism of interactions, and both Langmuir and Freundlich models manifested good consistency with the experimental data [10]. The removal of Pb ions was also investigated using fish scales as adsorbent. The effect of the adsorbent porosity and the feed rate were studied. A numerical model has been developed to describe the experiment taking into account the adsorption coefficient at neutral pH [14]. Other recycled materials from wool were also tested as potential adsorbents for Pb ions and the obtained results showed a good selectivity with different adsorption rates [15].

Alternatively, researchers showed that a variety of materials of plant origin had the ability to fix large quantities of heavy metals [16–20], in particular date stones [21–27]. It is necessary to note that significant amounts of date stones are generated each year and are identified as an important source of agricultural waste. It is therefore a wise choice from economic interest to transform such abundant and low-cost biowaste into added value product, for instance as potential adsorbent for heavy metal ions.

Moreover, several studies have proven the effectiveness of ultrasound during the adsorption process [28–35]. It has been used to facilitate the interaction between adsorbate and adsorbent, as consequence an enhanced adsorption process associated with faster chemical processes through the formation of acoustic cavitation due to the propagation of pressure waves through liquid [36]. Also, ultrasound, by means of cavitation phenomenon, enhances the mass transfer rate and may cause the formation of many micro-cracks on the solid surface hence increasing the surface area between solid–liquid in separation operation [30].

The aim of this work is to eliminate lead ions from aqueous solutions by adsorption on a support obtained from natural by products; i.e. date stones. This choice is mainly manifested by economic consideration, because raw materials and synthesis techniques are time consuming, complex and require toxic reagents besides being non-benign towards environment. In this perspective, this research consists on: (i) transformation of biowaste date stones into carbonized and subsequently activated products; (ii) optimization of operational conditions to achieve high adsorption rate of Pb(II) by the as-obtained adsorbents; (iii) further enhancement of adsorption performance by means of ultrasound agitation.

2. Experimental part

2.1. Preparation of adsorbents based on date stones

The raw adsorbent was prepared as follow. Nuclei of dates were washed thoroughly with distilled water and then oven dried at 105 °C for 24 h. After that, they were grounded and sieved to retain the fraction between 0.5 and 2 mm [37]. The selected crushed date stones were introduced into closed porcelain capsules and subjected to carbonization in a muffle furnace (Nabertherm MO) at 800 °C for 1 h [38]. The obtained carbonized coal was placed in a beaker containing a 10 M nitric acid solution. The mixture was then stirred for 24 h then filtered through a

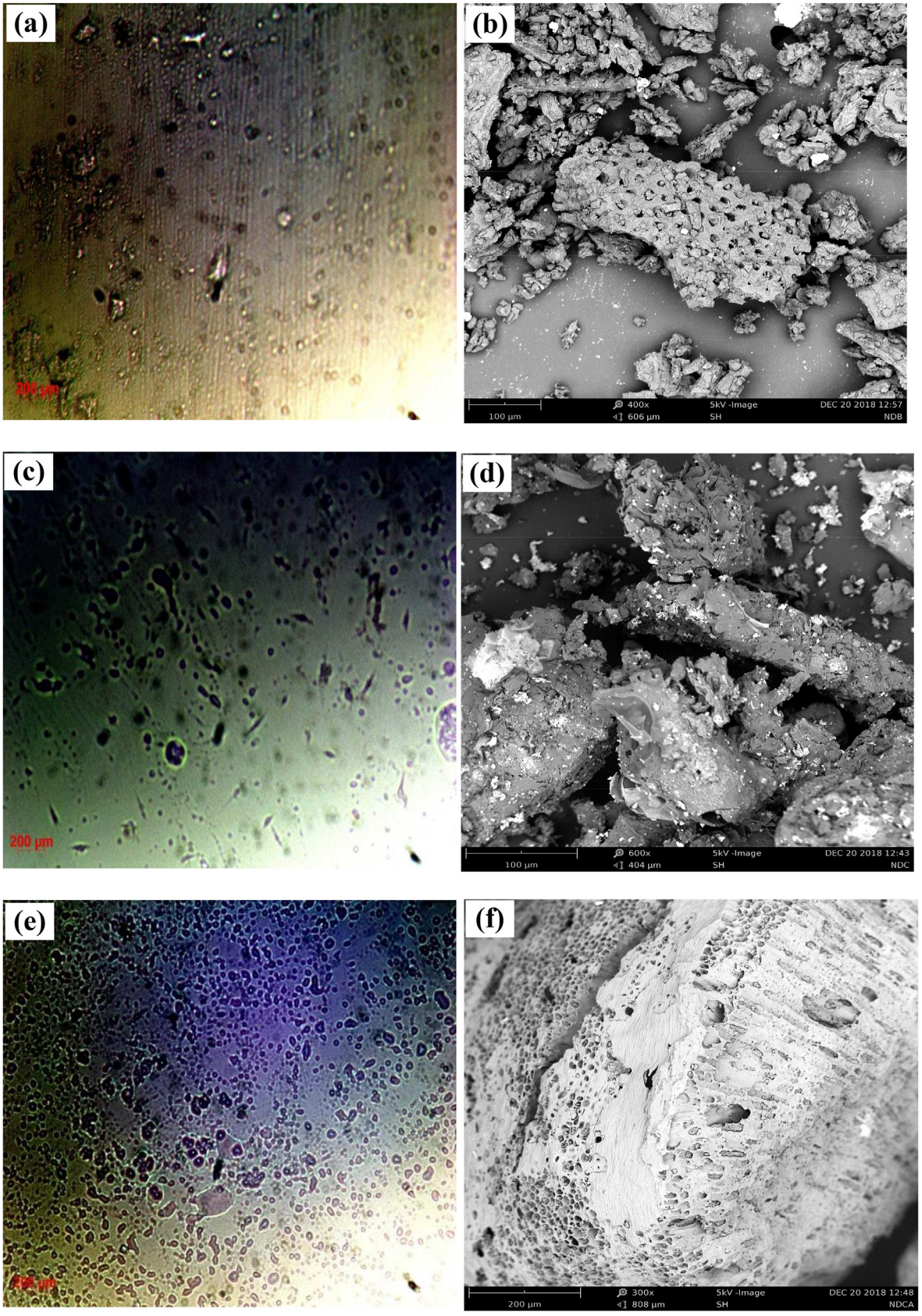

Fig. 2. Optical microscopy (a, c, e) and scanning electron microscopy (b, d, f) images for (a, b) RDS; (c, d) CDS; and (e, f) CADS adsorbents.

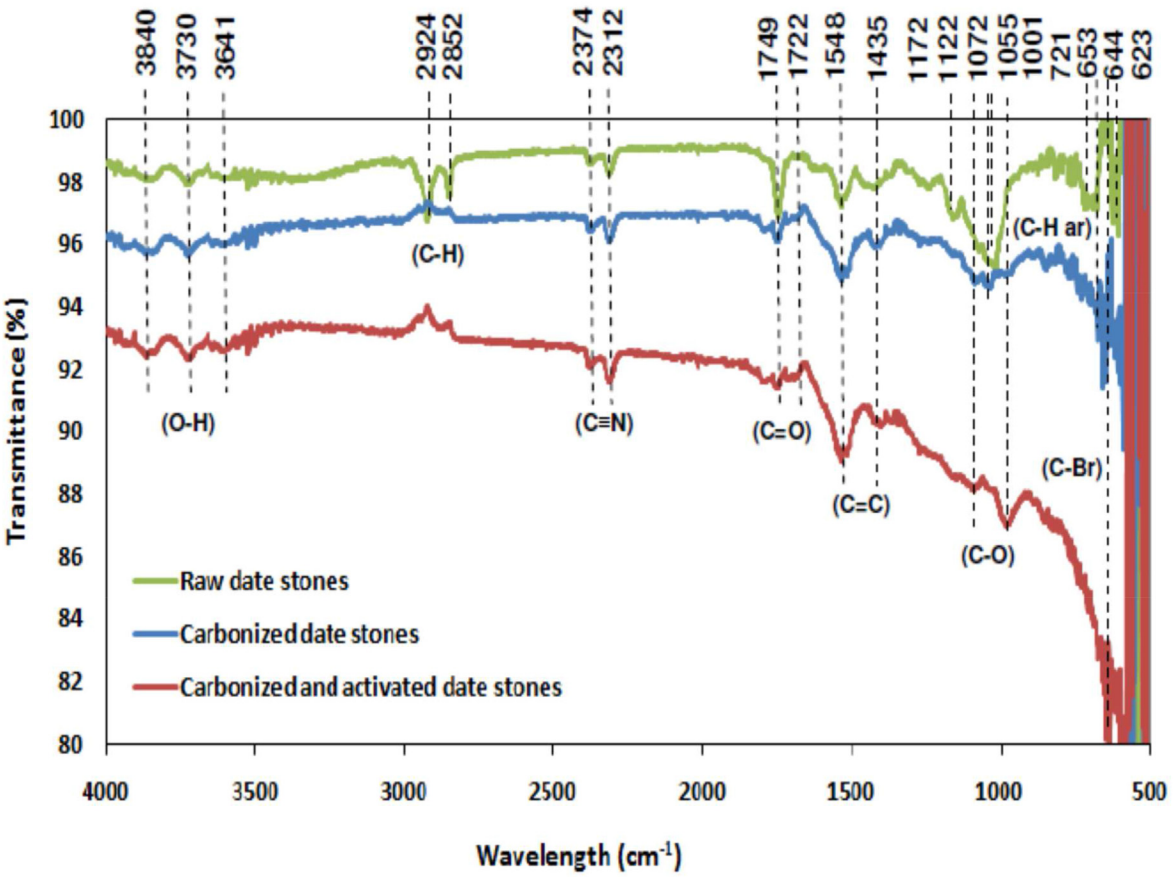

Fig. 3. FTIR spectra of RDS, CDS and CADS adsorbents.

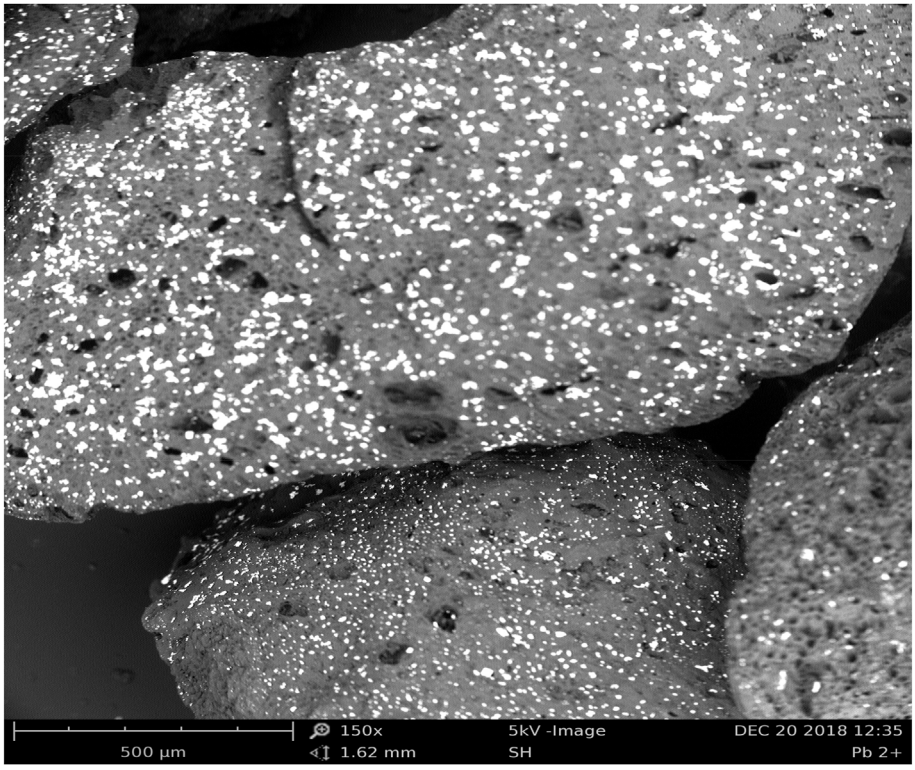

Fig. 4. SEM mage of CADS after Pb ions adsorption process.

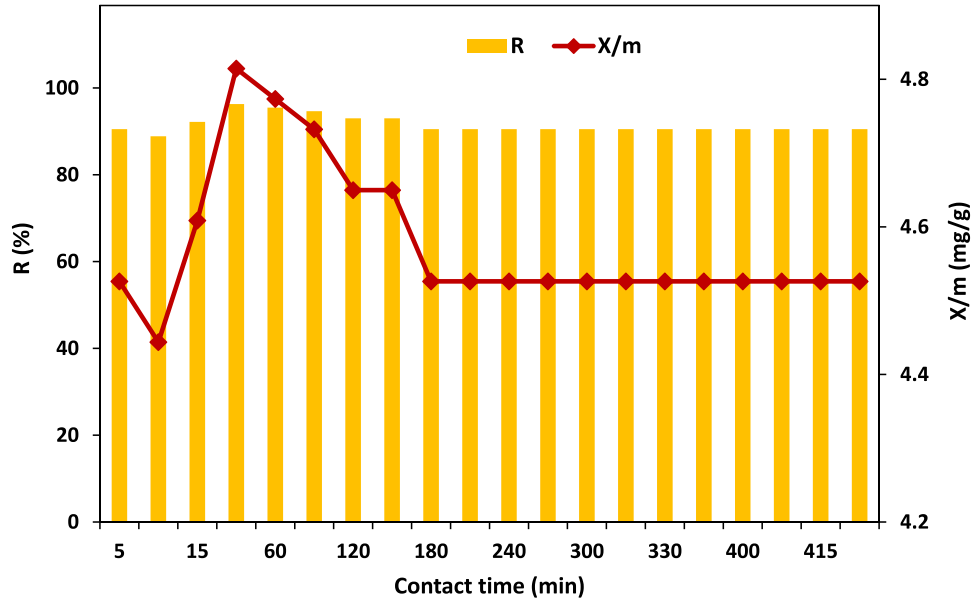

Fig. 5a. Adsorption kinetics of Pb ions on CADS. $[Pb^{2}+]_0 = 100$ mg/L; adsorbent mass = 0.5g; $V_{soluion} = 25$ mL; stirring speed = 500 rpm; pH = 5.6 ± 0.2; T = 18 ± 2 °C.

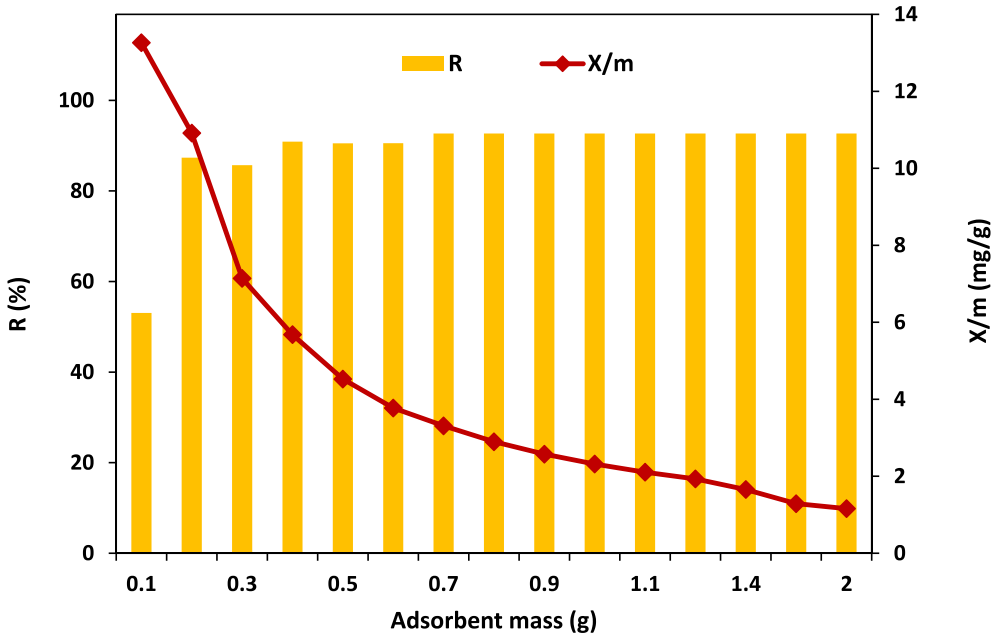

Fig. 5b. Influence of the adsorbent mass on the adsorption of Pb ions on CADS. $[Pb^{2}+]_0 = 100$ mg/L; $V_{soluion} = 25$ mL; stirring speed = 500 rpm; contact time = 3 h; pH = 5.6 ± 0.2; T = 18 ± 2 °C.

filter paper of 100 mm size. The final product "activated carbon" was washed thoroughly with distilled until a neutral pH and dried in an oven at 105 °C for 48 h.

In this study, three adsorbents were investigated, namely: raw date stones "RDS", carbonized date stones "CDS", and carbonized/activated date stones "CADS".

2.2. Preparation of solutions

To determine the Pb(II) concentration; EDTA solutions have been prepared with selected concentrations that allow a sufficient complexation of the metal ions and a buffer solution (pH = 10) was prepared from a solution of ammonium hydroxide NH4OH (0.1 N) and a solution of ammonium chloride NH4Cl (0.1 N).

The adsorption solutions were prepared from a single salt $Pb(NO_3)_2$ and from a mixture of electrolytes containing $Pb(NO_3)_2$ with $Co(NO_3)_2.6H_2O$. All reagents were supplied by Fisher Scientific-USA. The pH of solutions was adjusted with NaOH and HNO3. All solutions were prepared from analytical grade products and distilled water.

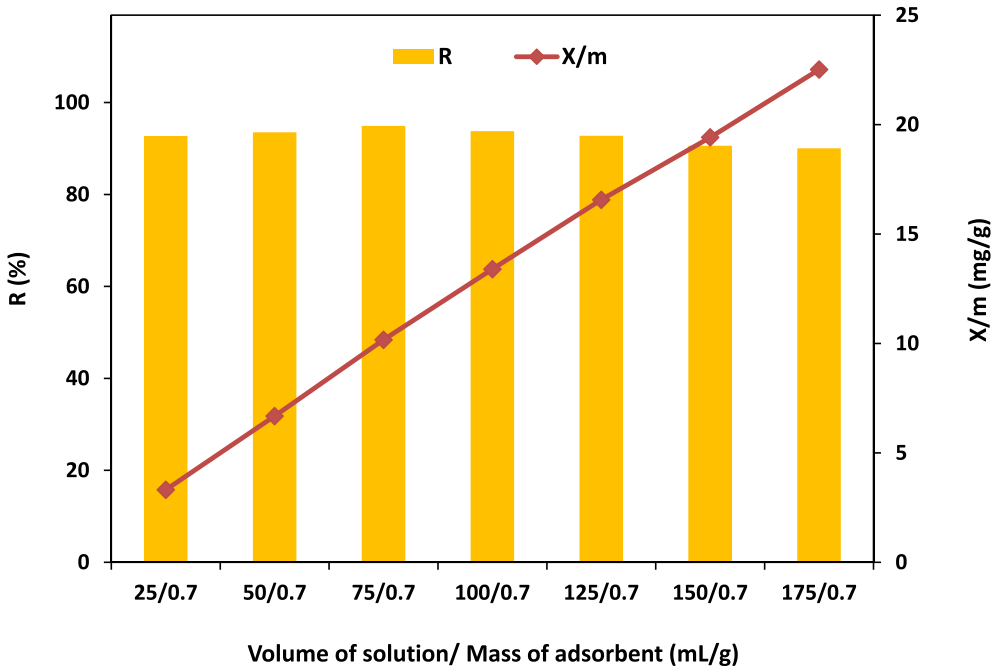

Fig. 5c. Effectof volume solution to mass adsorbent ratio on the adsorption of lead ions on carbonized and activated date stones "CADS". $[Pb^{2}+]_0$ = 100 mgL-1; adsorbent mass = 0.7g; stirring speed = 500 rpm/min; contact time = 3 h; pH = 5.6 ± 0.2; T = 18 ± 2 °C.

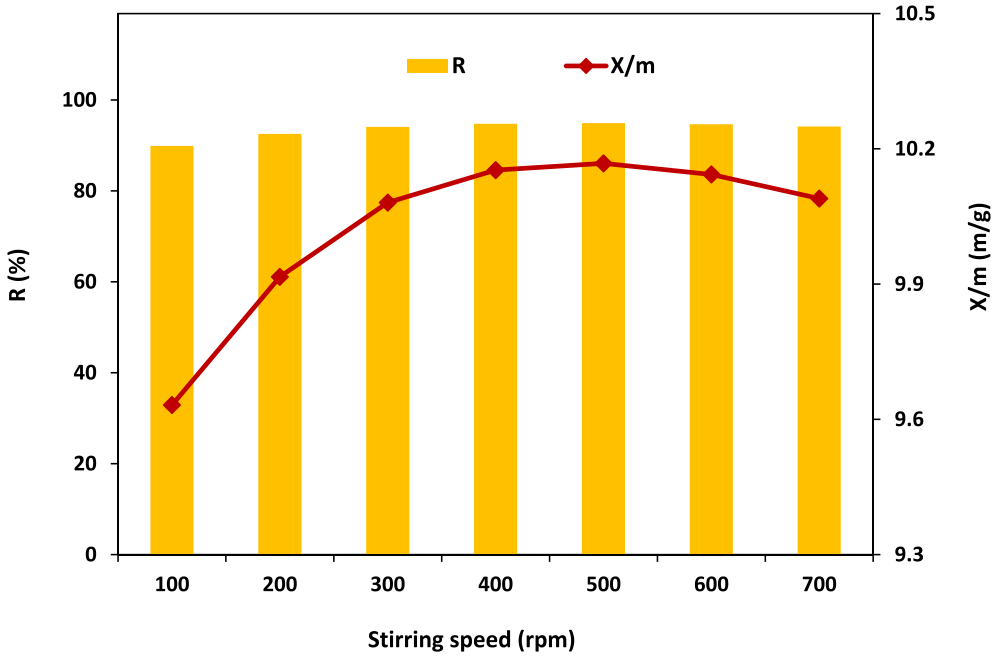

Fig. 5d. Effect of the agitation rate on the adsorption of Pb ions on CADS. $[Pb^{2}+]_0$ = 100 mg/L; adsorbent mass = 0.7g; $V_{soluion}$ = 75 mL; contact time = 3 h; pH = 5.6 ± 0.2; T = 18 ± 2 °C.

2.3. Adsorption of Pb(II) from aqueous solution by date stones

Amounts of adsorbent were mixed with volumes of solutions containing Pb(II) at a concentration of 100 mg/L. The mixtures were stirred on a multi-station magnetic stirrer for a well-defined contact time. The pH of the solutions was adjusted from 2 to 7 ± 0.2. At the end of the adsorption process, the solutions were filtered and centrifuged at 5000 rpm for 30 min to ensure the separation of adsorbent fine solid particles.

The analysis of Pb(II) in the filtrates was performed by UV–Visible spectrophotometry (Jenway) at wavelength of 240 nm using EDTA as complexing agent at pH 10.

The adsorption rate of Pb(II) (R%) was calculated as follow:

$$R(\%) = \frac{C_0 - C_e}{C_0} \cdot 100 \quad (1)$$

where C_0 and C_e represent respectively the initial and equilibrium Pb(II) concentrations.

The amount of the adsorbed metal q_e is given as follow:

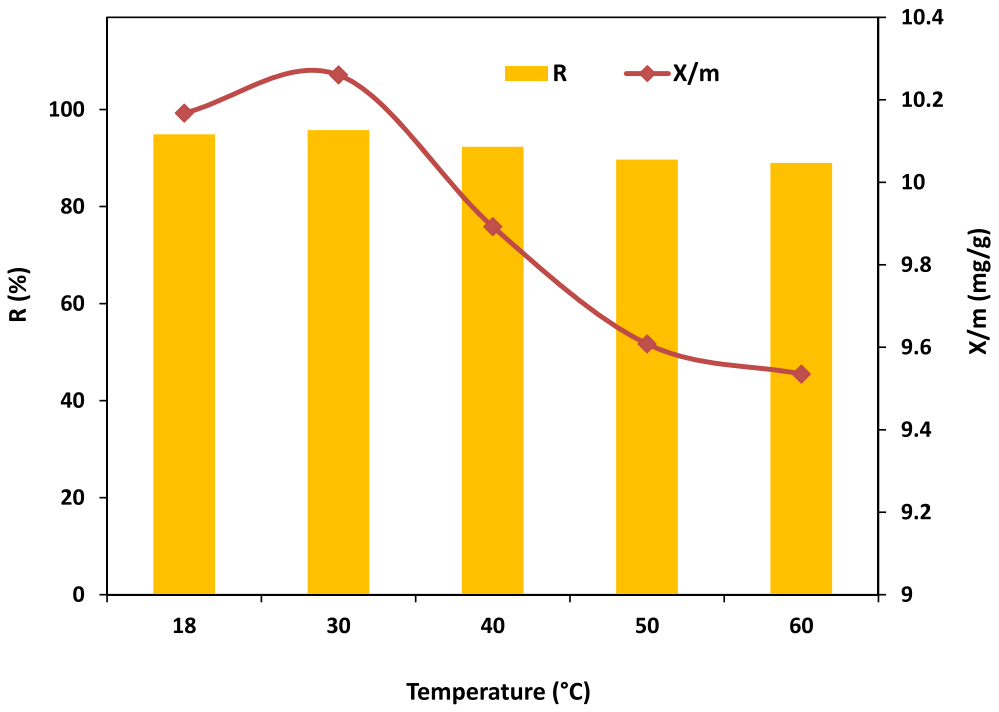

Fig. 5e. Effect of temperature on the adsorption of Pb ions on CADS. $[Pb^{2}+]_0 = 100$ mg/L; adsorbent mass = 0.7g; $V_{soluion} = 75$ mL; contact time = 3 h; stirring speed = 500 rpm/min; pH = 5.6 ± 0.2.

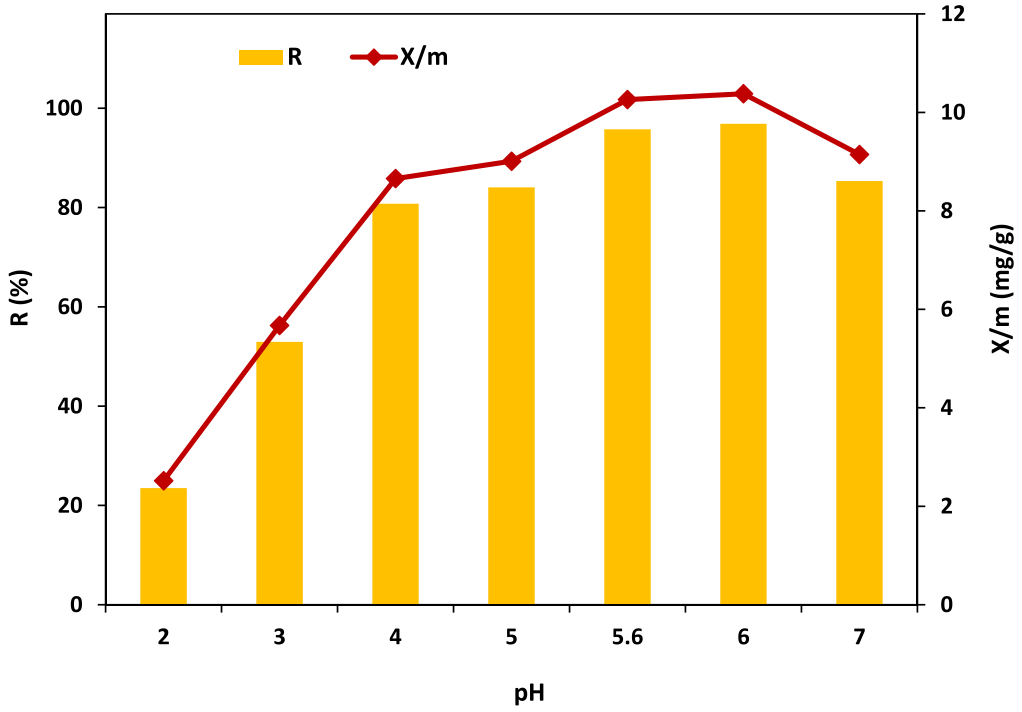

Fig. 5f. Effect of pH solution on the adsorption of Pb ions on CADS. $[Pb^{2}+]_0 = 100$ mg/L; adsorbent mass = 0.7g; $V_{soluion} = 75$ mL; contact time = 3 h; stirring speed = 500 rpm/min; T = 30 °C.

$$q_e = \frac{X}{m} \quad (2)$$

where m represents the weight of the solid sample and X is defined as follows [26]:

$$X = (C_0 - C_e) \cdot V \quad (3)$$

where V represents the volume of solution.

To improve the adsorption efficiency of Pb(II) on the activated carbon derived from date stones, some operational conditions were optimized;

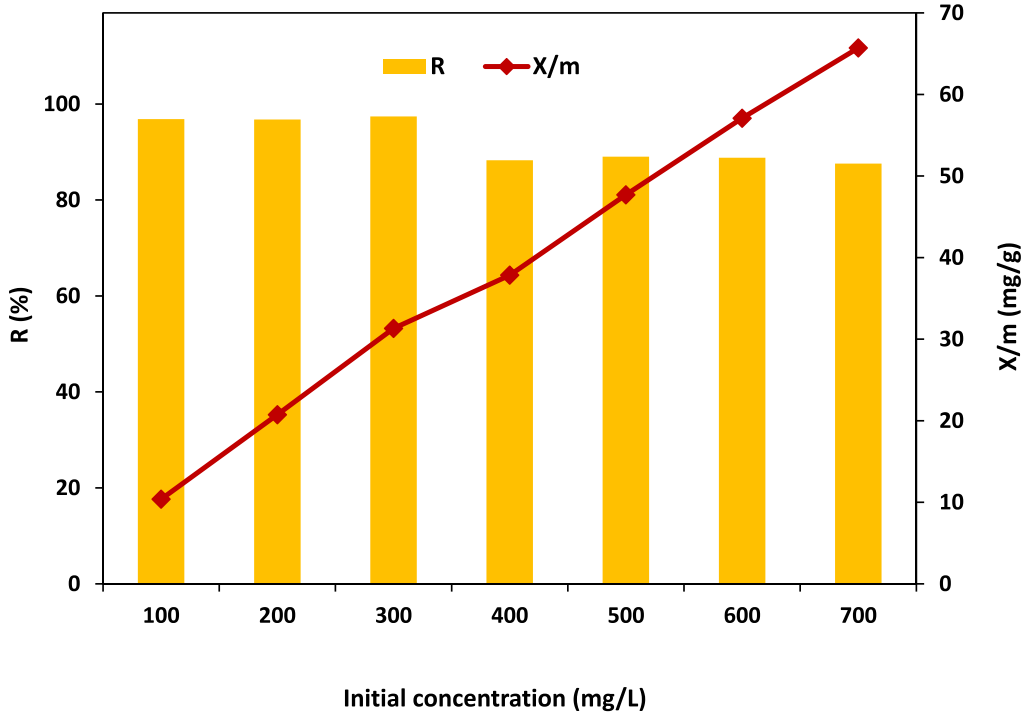

Fig. 5g. Effect of the initial concentration of Pb ions on their adsorption on CADS. Adsorbent mass = 0.7g; $V_{soluion}$ = 75 mL; contact time = 3 h; stirring speed = 500 rpm/min; T = 30 °C; pH = 6.

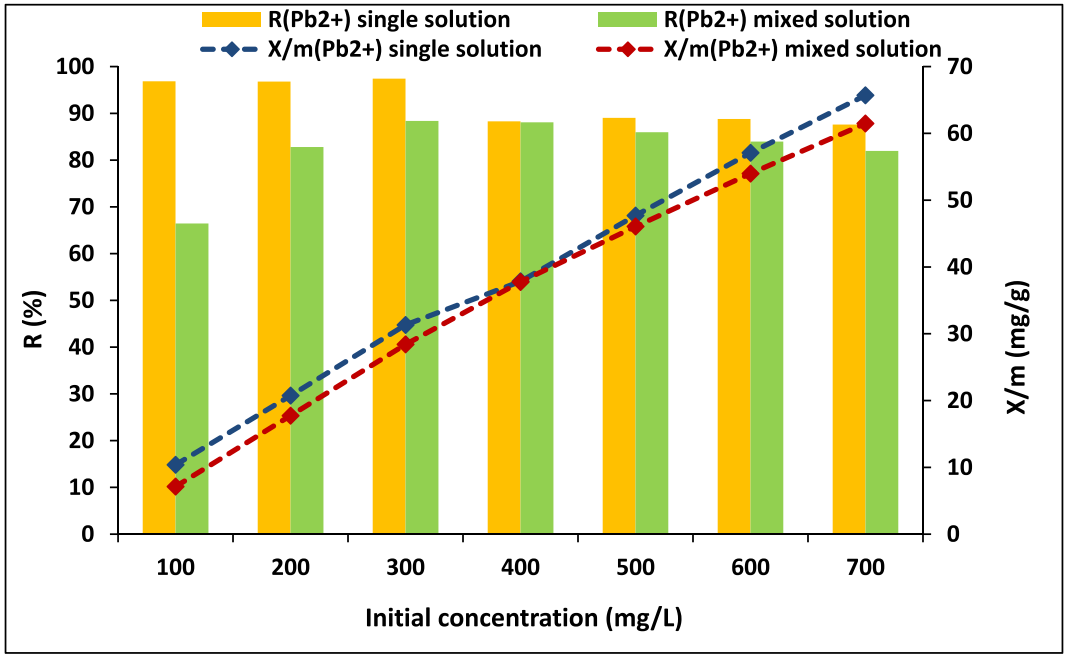

Fig. 6a. Adsorption rate of Pb ions on CADS in single and mixed solutions. $[Pb^{2+}]_0 = [Co^{2+}]_0$. Adsorbent mass = 0.7g; $V_{soluion}$ = 75 mL; contact time = 3 h; stirring speed = 500 rpm/min; T = 30 °C; pH = 6.

nature of adsorbent, contact time, mass of adsorbent, volume solution to mass adsorbent ratio, stirring speed, temperature, pH of solution, and initial concentration of Pb(II).

The adsorption on activated carbon prepared from date stones was also studied for a mixed solutions containing Pb(II) and Co(II) (cobalt ions) at equimassic concentration, corresponding to an equivalent molar concentration of Co(II) equal to 3.5 times of Pb(II). In fact, this ratio reflects the real concentrations of industrial discharges from some iron and steel industries in Algeria.

A comparative study has been carried out by varying the initial concentration of Pb(II) in the feed solutions. For each concentration, two types of activated carbon were tested; derived from date stones "CADS"

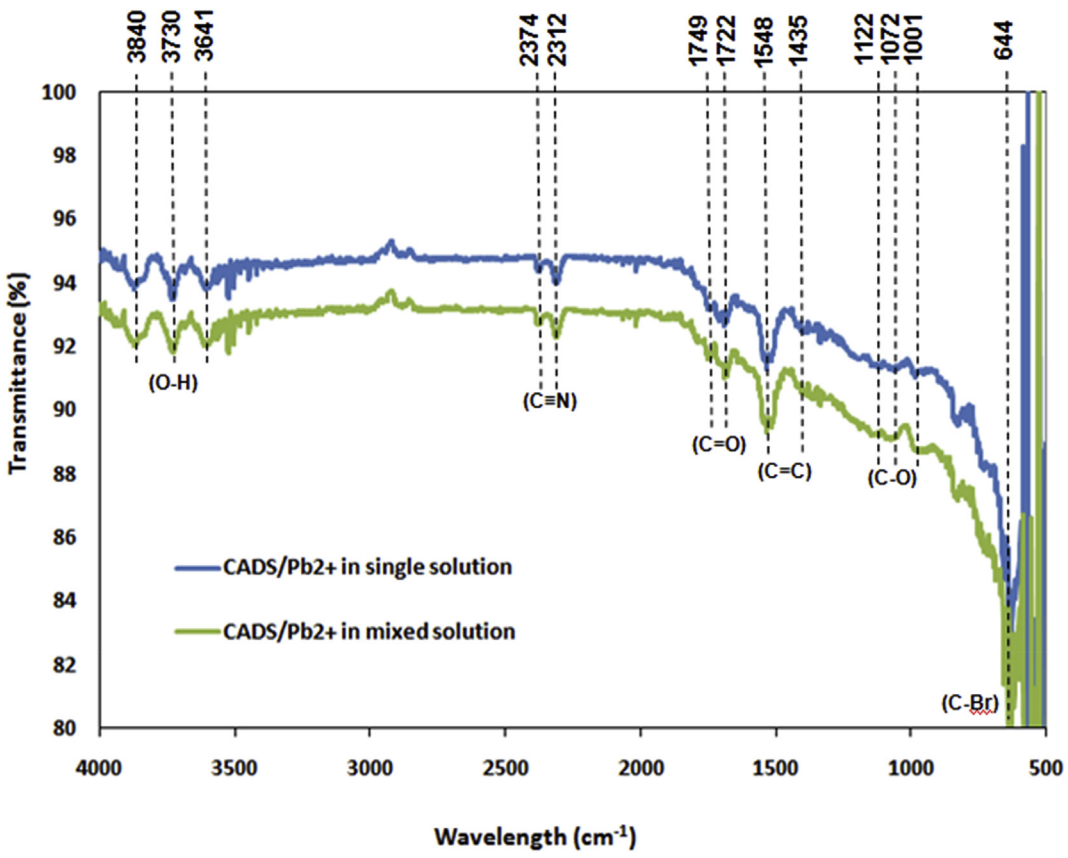

Fig. 6b. FTIR spectra of CADS after adsorption of Pb ions in single and mixed solutions. Adsorbent mass = 0.7g; $V_{soluion}$ = 75 mL; contact time = 3 h; stirring speed = 500 rpm/min; T = 30 °C; pH = 6.

and a commercial activated carbon "CAC". The operational parameters were fixed according to the previously optimized operational conditions.

To further improve the adsorption efficiency, ultrasound radiation was utilized by investigating the effects of sonolysis time and temperature. Experiments were performed using an ultrasonic bath (Elmasonic S 60 H) at a frequency of 37 kHz and a power of 550 W.

The concentration of Pb(II) was determined at the wavelength of 240 nm using EDTA as chelating agent at pH = 10.0, knowing that at this wavelength the complex of EDTA with Co(II) gives almost zero absorbance.

In this study, the adsorption measurements were carried out in triplicate and the estimated errors was estimated to be around 5%.

2.4. Characterization of adsorbents

The surface morphology of the as-prepared adsorbents were analyzed by optical microscopy (OM) using a Zeiss Axio Imager M1 Trinocular Frame optical microscope (Germany) and scanning electron microscopy (SEM) using a PHENOM PURE scanning electron microscope (Netherlands). The functional groups before and after Pb(II) adsorption were determined by Fourier transform infrared (FTIR) spectroscopy using IRAffinity-1S Shimadzu combined with a single reflection ATR spectrophotometer (Germany).

The specific surface area of the adsorbents was measured by determining the methylene blue (MB) index [39]. This method is based on the adsorption of MB molecules in the pores of the adsorbent for a specific contact time of a given amount of adsorbent with a solution of a known MB concentration. The maximum quantity of adsorbed MB will be used to estimate the specific surface area of the adsorbent covered by MB molecules.

3. Results and discussion

3.1. Optimization of operational conditions of Pb(II) adsorption on activated carbon prepared from date stones

A preliminary study has been performed in order to examine the adsorption capacity of the chosen material; i.e. activated carbon prepared from date stones to achieve the optimum efficiency under given operational conditions.

3.1.1. Effect of adsorbent nature

The adsorption rate of Pb(II) on three types of adsorbents (Fig. 1), has proved that the optimum efficiency was obtained for CADS (R = 90.47%; X/m = 4.52 mg/g) in comparison with CDS (R = 81.65%; X/m = 4.08 mg/g) and RDS (R = 70.03%; X/m = 3.50 mg/g).

These results are expected when considering that both carbonization and activation processes are known to improve the physico-chemical properties of the as-treated raw materials particularly the specific surface area besides the creation of more active sites hence an enhancement of the adsorption efficiency. This finding is greatly supported by substantial increase in the specific surface area; i.e. 128.8, 203.9 and 244.7 m^2/g for RDS, CDS and CADS respectively.

The optical microscopy images displayed in Fig. 2 (a, c, e) indicate that RDS, CDS and CADS have similar morphology with the development of an important porous texture following the carbonization and chemical activation processes. This has been further evidenced by SEM observations as shown in Fig. 2 (b, d, f) where both carbonized and activated samples result in high porosity over the entire surface of the particles with some heterogeneity. Fig. 2b reveals that the ground material (raw date stones) is formed from agglomerates of fine particles besides large particles forming such typical network microstructure. After

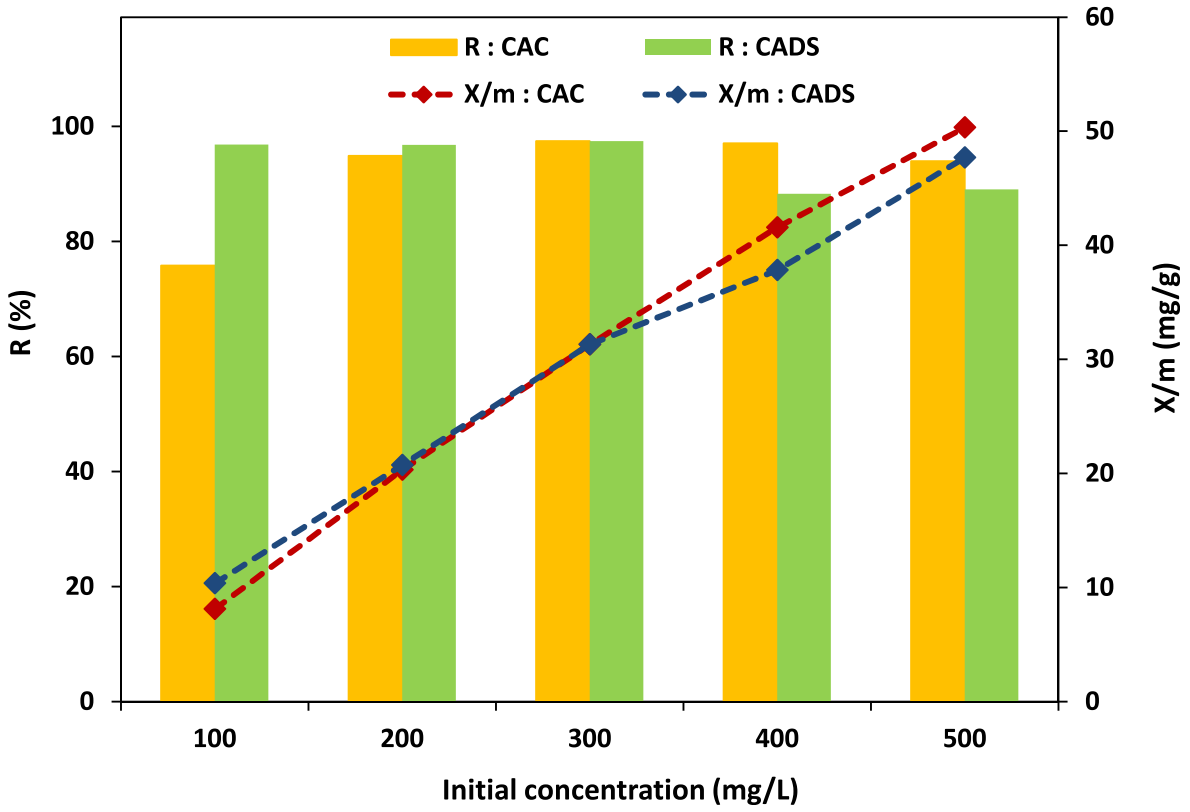

Fig. 7. Adsorption of Pb ions on CAC and CADS by varying the initial concentration of Pbions. Adsorbent mass = 0.7g; $V_{soluion}$ = 75 mL; contact time = 3 h; stirring speed = 500 rpm/min; T = 30 °C; pH = 6.

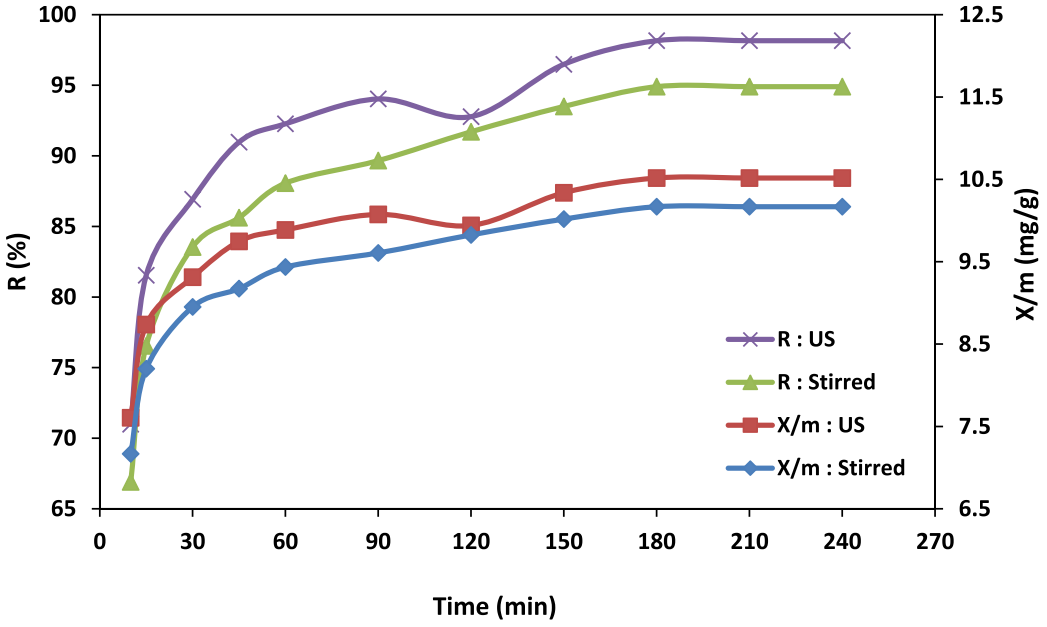

Fig. 8a. Effect of sonolysis time on the adsorption of Pb ions on CADS assisted with ultrasound compared to stirred batch. [Pb2+]0 = 100 mg/L; adsorbent mass = 0.7 g; Vsoluion = 75 mL; stirring speed = 500 rpm/min; T = 18 ± 2 °C; pH = 5.6 ± 0.2.

carbonization, some cavities appear on the surface (Fig. 2d) which become more important following the activation process as consequence of the release of the cavities filled with tar (Fig. 2f).

FTIR spectral analysis shows that RDS, CDS and CADS adsorbents have similar chemical structure (Fig. 3), except some difference in the bands' positions (shift) and relative intensity due to the different treatments which can minimize the functional groups formed on the surface of the adsorbent particles. The spectra corresponding to RDS, CDS and CADS display peaks at 623, 653 and 644 cm^{-1} respectively, assigned to C–Br stretching vibration bond of bromoalkanes. The peak appeared at

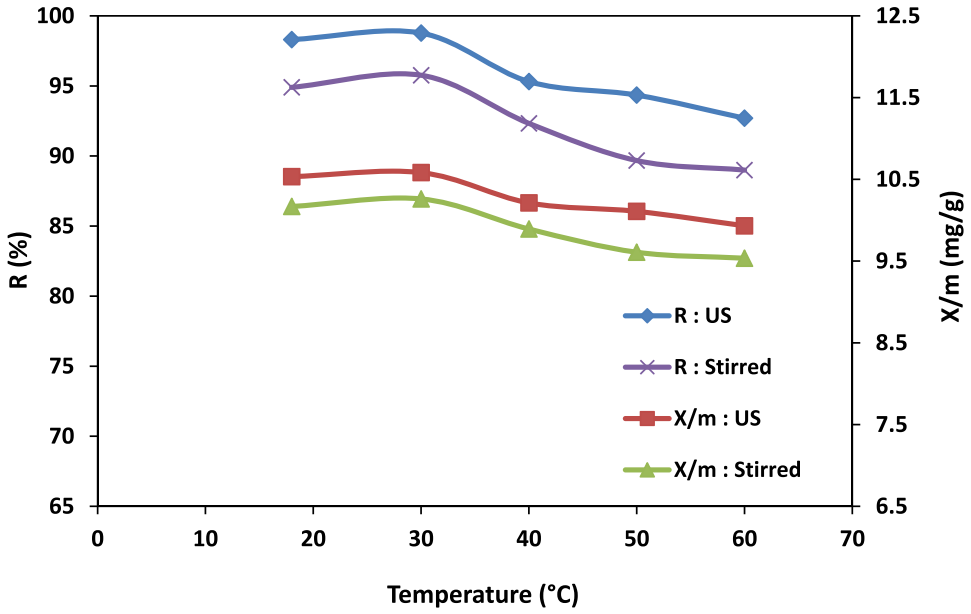

Fig. 8b. Effect of temperature on the adsorption of Pb ions on CADS assisted with ultrasound compared to stirred batch. [Pb2+]0 = 100 mg/L; adsorbent mass = 0.7 g; Vsoluion = 75 mL; sonolysis and contact time = 3 h; stirring speed = 500 rpm/min; pH = 5.6 ± 0.2.

721 cm^{-1} for RDS can be attributed to C–H aromatic bond. The two peaks observed at 1055 and 1172 cm^{-1} (RDS), 1001 and 1072 cm^{-1} (CDS) and 1001 and 1122 cm^{-1}(CADS), are characteristics of the stretching vibrations of C–O bonds belonging to alcohol and phenol functions. For the three adsorbents, others peaks have been detected; two bands at 1435 and 1548 cm^{-1} ascribed to C═C stretching vibrations of alkenes, two bands at 1749 and 1722 cm^{-1} attributed to C═O stretching vibration bonds, and two bands at 2312 and 2374 cm^{-1}corresponding to C≡N bonds. For the RDS spectrum, additional peaks appear at 2852 and 2924 cm^{-1} which can be associated with C–H bond. Furthermore, common peaks are detected at 3641, 3730 and 3840 cm^{-1}, which are assigned to the free O–H bonds, originating from to alcohols or carboxylic acids and/or to simple hydroxyls belonging to the free water bound to adsorbents surface.

Fig. 4 presents an SEM image of CADS after Pb(II) adsorption process, it clearly highlights the presence of white spots (heavy elements appear brighter compared to lighter elements since SEM contrast depend on the atomic number) homogenously distributed over the entire agglomerates, there by proving the fixation of metal cations on the adsorbent surface compared to that before adsorption in Figure 2f.

Based on the results obtained following the preliminary adsorption tests alongside SEM and FTIR characterizations, activated charcoal (i.e. carbonized and activated date stones - CADS) has been selected for further studies.

3.1.2. *Effect of contact time*

Fig. 5a illustrates the evolution of the adsorption capacity of Pb(II) by CADS as function of contact time. A typical characteristic trend is observed, a gradual increase until reaching an equilibrium stage known as saturation. This phenomenon can be explained by the diffusion of Pb ions to the adsorption sites to reach adsorption equilibrium where all sites become occupied and manifest similar behavior towards Pb ions. The same tendency was observed with other comparable sorbent-metal systems [40–42]. The adsorption of Pb ions becomes stable after 180 min where a steady state is established, estimated as R = 90% (X/m = 4.53 mg/g) for a Pb(II) concentration of 100 mg/L and a natural pH (5.6 ± 0.2).

3.1.3. *Effect of the adsorbent mass*

For an initial Pb(II) concentration of 100 mg/L and an equilibrium contact time of 180 min, it is noted that the adsorption rate varies considerably when changing the CADS adsorbent mass from 0.1 to 2.0 g, see Fig. 5b. Indeed, the adsorption rate almost doubled from 53% for up to 93% for 0.1 g and 0.7 g respectively, then reached a steady state. This is in good agreement with [43]. Meanwhile, the adsorbed quantity of Pb ions decreases significantly from 13.26 mg/g for 0.1 g up to 1.16 mg/g for 2.0 g. This decrease is expected, because the smaller the quantity of adsorbent, the more saturated it will be for the same quantity of solute, but the rate and kinetics of adsorption are strongly dependent on the intrinsic (selectivity) and extrinsic (such as surface area) characteristics the adsorbent alongside the optimized operational parameters.

3.1.4. *Effect of (solution volume)/(adsorbent mass) ratio*

For a fixed amount of CADS adsorbent (0.7 g) while varying the solution volume from 25 to 75 mL (Fig. 5c), it is noted that the adsorption capacity of Pb(II) increases gradually reaching a maximum value around 94.9%. This result can be explained by the fact that 0.7 g of adsorbent mass can provide more active sites for Pb ions, meanwhile their amount increases by increasing the solution volume. However, a rise in the solution volume beyond 75 mL for the same initial concentration (100 mg/L), results in a decline of the adsorption rate because the amount of Pb ions becomes more important as the adsorbent mass becomes insufficient to retain all of them. Accordingly, a solution volume of 75 mL corresponds to the optimum value for the adsorbent mass of 0.7g. Similarly, the adsorbed quantity gradually increases by increasing the solution volume; i.e. the value of X/m increases significantly from 3.31 mg/g for 25 mL up to 22.51 mg/g for 175 mL. This result can be explained by the fact that for the same adsorbent mass (0.7 g), a larger volume of the feed solution leads to an increase in the quantity of solute which in evidenced by a greater adsorbed amount of Pb(II) on the surface of adsorbent.

3.1.5. *Effect of stirring speed*

As can be seen in Fig. 5d, it is found that the highest capacity of Pb(II) removal by CADS occurred at an optimal agitation speed of 500 rpm/min; with R = 94.9% and X/m = 10.17 mg/g. The adsorption rate and the adsorbed amount increase with increasing the agitation speed from 100

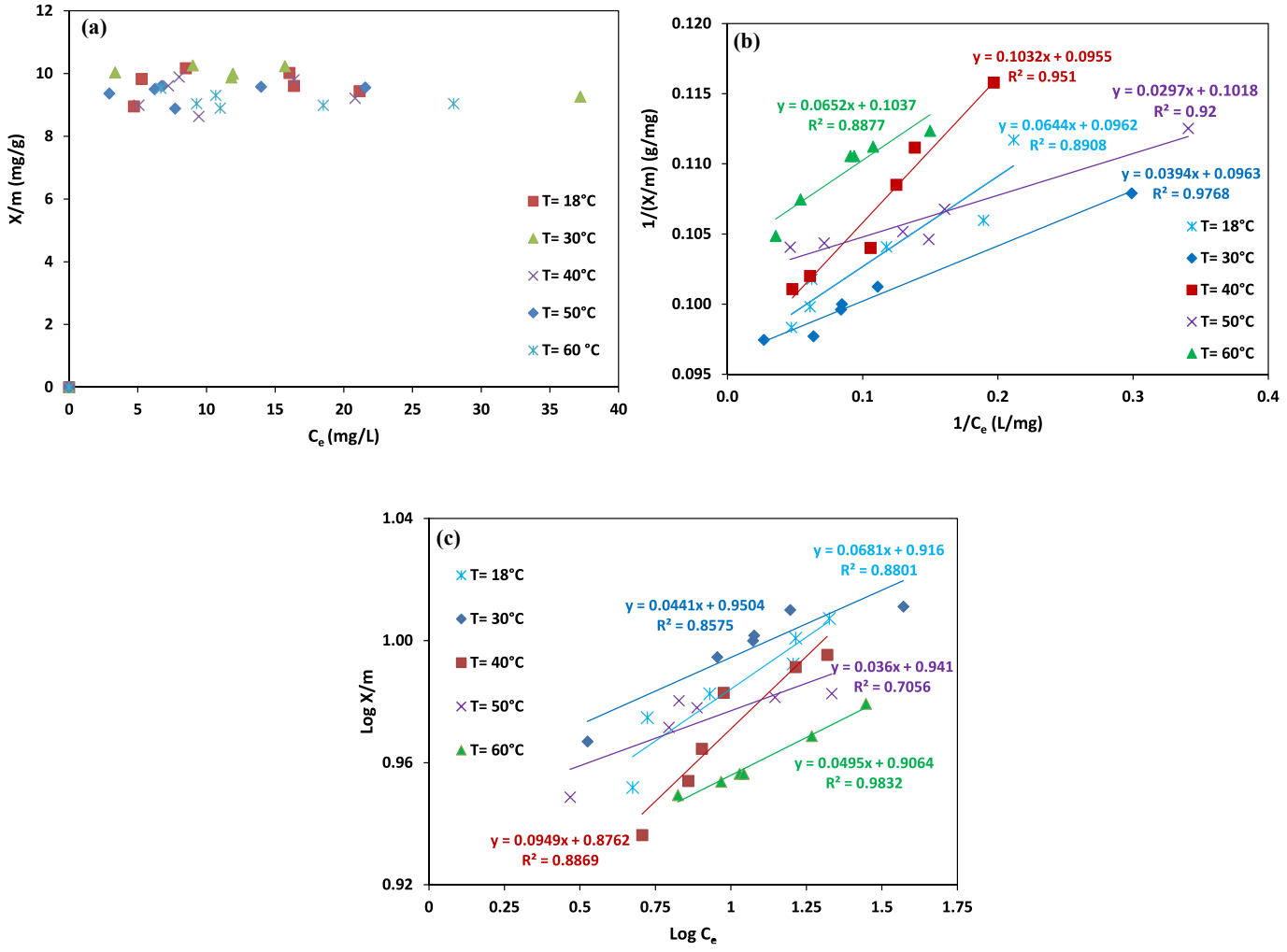

Fig. 9. Adsorption isotherms (a) and linearization of Langmuir (b) and Freundlich (c) models at different temperatures for the adsorption isotherms of Pb ions on CADS. [Pb2+]0 = 100 mg/L; adsorbent mass = 0.7 g; Vsoluion = 75 mL; stirring speed = 500 rpm/min; pH = 5.6 ± 0.2.

Table 1
Parameters of Langmuir and Freundlich models' for the adsorption of Pb ions on carbonized and activated date stones "CADS" at different temperatures.[Pb^{2+}] = 100 mg/L, volume of solution = 75 mL, mass of adsorbent = 0.7g, stirring speed = 500 rpm/min, pH = 5.6 ± 0.1.

Temperature (°C)	Langmuir model			Freundlich model		
	b (mg/g)	a (L/mg)	R^2	K_F	1/n	R^2
18	10.3950	1.4938	0.8908	8.2414	0.0681	0.8801
30	10.3842	2.4442	0.9768	8.9207	0.0441	0.8575
40	10.4712	0.9254	0.9510	7.5197	0.0949	0.8869
50	9.8232	3.4276	0.9200	8.7297	0.0360	0.7056
60	9.6432	1.5904	0.8877	8.0612	0.0495	0.9832

to 500 rpm. This phenomenon can be explained by the fact that the diffusion rate of solutes from the bulk liquid to the liquid boundary layer surrounding the adsorbent particles becomes faster because of a the enhancement of turbulence and a decrease of the thickness of the liquid boundary layer [44]. However, much higher agitation speed above the optimal value (600 and 700 rpm) generates the accumulation of solute ions on the surface of adsorbent particles and hence a concentration gradient is established between the solid and the bulk solution. Indeed, this concentration gradient favors the creation of a diffusion flow antagonistic to convection flow of the solution, which induces to a decrease in the adsorption rate.

3.1.6. *Effect of temperature*

The variation of the medium temperature from 18 to 30 °C has been found to have a direct impact on the adsorption rate of CADS; a maximum value of 95.76% is reached at a fixed Pb(II) amount of 10.26 mg/g (Fig. 5e). This means that the increase in temperature promotes ions kinetic energy thereby favoring their distribution homogeneously over the entire adsorbent particles surface. Indeed, it is well-known that the diffusion rate of the adsorbate solutes increases with the rise in the medium temperature, owing to the decrease in the viscosity of the solution [44]. However, when the medium temperature reaches the range 40–60 °C, it will cause a drop in the adsorption rate, because at higher temperature, the attractive forces between the adsorbent surface and metal ions are weakened and the adsorption decreases which supports physical adsorption. In addition, at high temperatures, the thickness of the

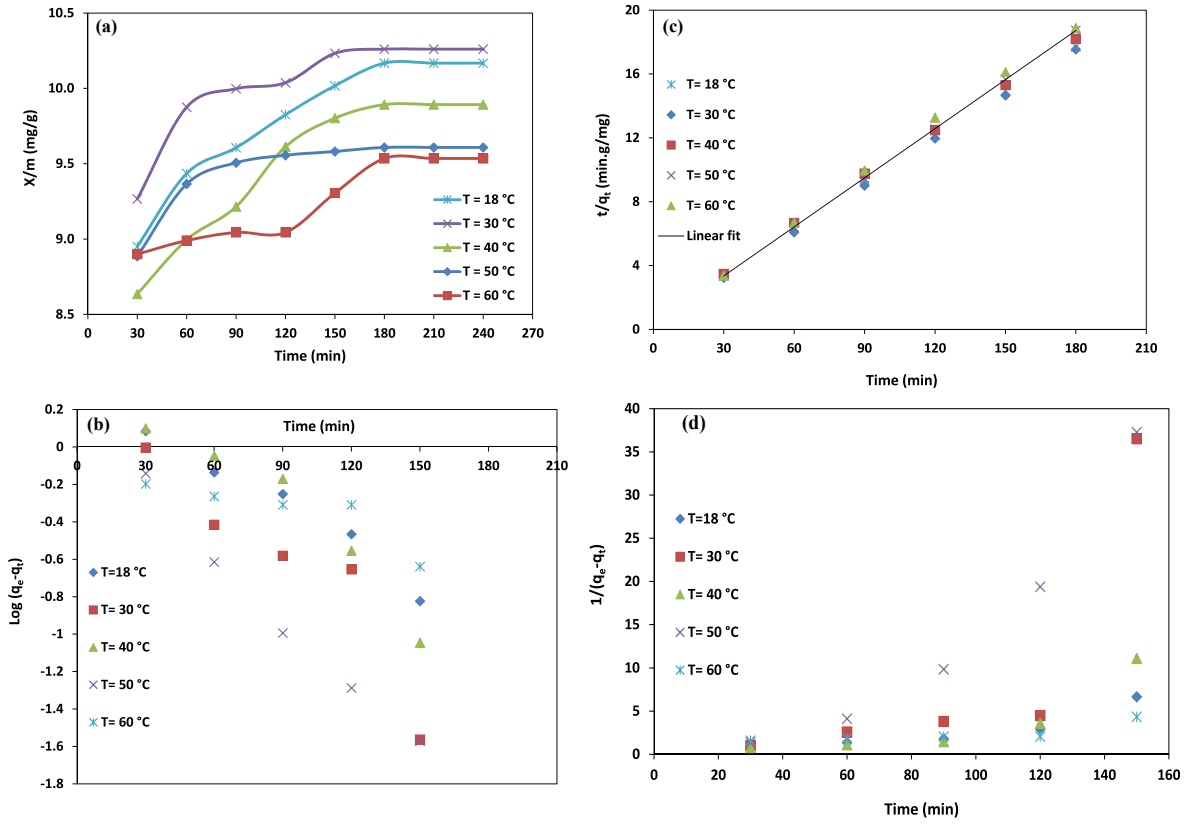

Fig. 10. Kinetic adsorption (a), First-order rate (b), Pseudo-second order rate (c) and Second-order rate (d) models for the adsorption of Pb ions on CADS. [Pb2+]0 = 100 mg/L; adsorbent mass = 0.7 g; Vsoluion = 75 mL; stirring speed = 500 rpm/min; pH = 5.6 ± 0.2.

Table 2
Models rate constants for Pb ions adsorption kinetics on carbonized and activated date stones "CADS". [Pb^{2+}] = 100 mg/L, volume of solution = 75 mL, mass of adsorbent = 0.7g, stirring speed = 500 rpm/min, pH = 5.6 ± 0.1.

Temperature (°C)	18	30	40	50	60
$q_{e\ exp}$ (mg/g)	10.1679	10.2603	9.8923	9.6081	9.5351
First order rate model					
$q_{e\ cal}$ (mg/g)	2.1198	2.3153	3.1311	1.3750	0.8608
k_L (1/min)	0.0166	0.0258	0.0214	0.0271	0.0071
R^2	0.9655	0.8595	0.9187	0.9873	0.7343
Pseudo-second-order rate model					
$q_{e\ cal}$ (mg/g)	10.4493	10.4712	10.2669	9.7561	9.6154
k'(g/mg.min)	0.0148	0.0235	0.0125	0.0389	0.0236
R^2	0.9995	0.9999	0.9992	0.9999	0.9984
Second-order rate model					
$q_{e\ cal}$ (mg/g)	–	–	–	–	1.5584
k (g/mg.min)	0.0441	0.2433	0.0770	0.2903	0.0192
R^2	0.8003	0.5862	0.7118	0.8978	0.6535

boundary layer surrounding the adsorbent particles decreases due to the excessive leakage of solutes from the surface of the biomaterial to the solution which leads to a decrease in the adsorption [45].

3.1.7. Effect of pH

It has been reported that the removal of Pb ions by adsorption is highly dependent on the pH of the aqueous solution; hence this parameter has been examined in detail for CADS. During the experimental study, the pH of the solution has been varied from 2 to 7 after determining the pH at zero charge point of the adsorbent (pHpzc = 5.8), where the net charge on the surface of the adsorbent is zero. This parameter is very important in adsorption phenomena, especially when electrostatic forces are involved in the mechanisms. A quick and easy way to determine the pHPZC of the adsorbent consists on mixing 1 g of solid with 20 cm of CO2-free distilled water. The slurry is kept in a plastic bottle and shaken periodically for one or two days until the pH is stabilized, taking the final pH of the slurry as the pHPZC of the solid [46]. The results for the different pH values are shown in Fig. 5f. As the pH of the solution drops, the surface of adsorbent is positively charged (pH < pHPZC) which will not promote the adsorption of positively charged metal cations due to the electrostatic repulsion. At pH = 2, the medium is strongly acidic and the adsorption is negligible (around 20%) because the number of positively charged surface sites increased, leading to electrostatic repulsion between the adsorbent surface and Pb cations. Furthermore, this finding can be explained by the fact that the concentration of protons H+ is high in solution which induces a competition with Pb(II) ions for the free active sites available at the surface of the adsorbent [47]. At pH = 6, the adsorbent becomes very effective for the elimination of Pb ions from the aqueous solution reaching a maximum rate (R = 96.86% and X/m = 10.38 mg/g) due to the attractive forces between Pb cations and the negatively charged surface of the adsorbent. At pH = 7, the adsorption rate decreases as we begin to approach the pH value corresponding to the precipitation of lead ions due to their transformation to the various hydrolysis products, namely $Pb(OH)^+$ and/or $Pb(OH)_2$ which are less or not retained by the adsorbent [48].

3.1.8. Effect of initial concentration

The adsorption process was found to be greatly influenced by the initial concentration of lead ions in the aqueous solution. Fig. 5g highlights that the adsorption capacity increases significantly when the initial concentration varies in the range 100–300 mg/L, reaching a maximum value of about 97.43% for [Pb+2]0 = 300 mg/L (X/m = 31.32 mg/L). This can be attributed to the attractive forces between the lead ions which are positively charged and the surface of CADS which becomes negative at the pH of the experiment (pH = 6 > pHPZC). An increase in the initial concentration of metal ions beyond 300 mg/L in solution

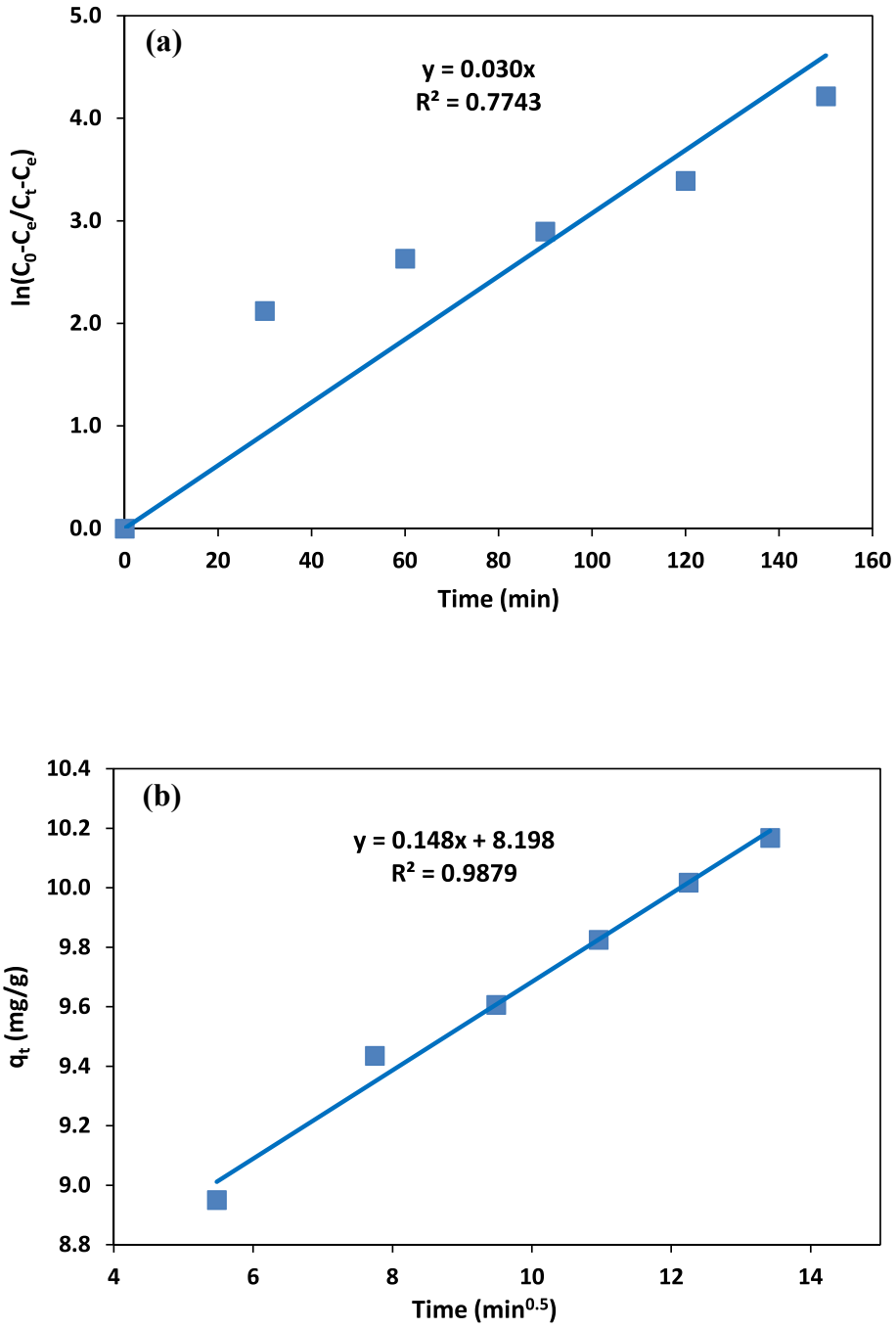

Fig. 11. External diffusion (a) and internal diffusion (b) models for the adsorption of Pb ions on CADS. [Pb2+]0 = 100 mg/L; adsorbent mass = 0.7 g; Vsoluion = 75 mL; stirring speed = 500 rpm/min; pH = 5.6 ± 0.2; T = 18 ± 2 °C.

Table 3
Diffusion parameters of Pb ions adsorption kinetics on carbonized and activated date stones "CADS". [Pb^{2+}] = 100 mg/L, volume of solution = 75 mL, mass of adsorbent = 0.7g, stirring speed = 500 rpm/min, pH = 5.6 ± 0.1.

Temperature (°C)	18	30	40	50	60
External diffusion					
k_{ex}	0.0307	0.0393	0.0319	0.029	0.0448
R^2	0.7743	0.8429	0.8737	0.3505	0.8451
Internal diffusion					
K_{in}($m.L^{-1}.min^{-0,5}$)	0.1486	0.1156	0.1667	0.0715	0.0837
C	8.1981	8.8026	7.7105	8.4296	8.5899
R^2	0.9879	0.879	0.9858	0.7860	0.8080

causes a slight decrease in the retention capacity. The same trend was noticed by Alghamdi et al., when they investigated the adsorption of lead ions on polypyrrole-based activated carbon. The authors have explained this behavior by the fact that the presence of a higher amount of adsorbate per unit mass of adsorbent may restrict the adsorption process [49].

Otherwise, the presence of a large number of Pb(II) leads to a screening of the negative charges of adsorbent and therefore repulsion is generated between the surface and Pb cations. The amount of Pb(II) adsorbed at equilibrium increased from 10,38 mg/L to 65.7 mg/L as the concentration was increased from 100 to 700 mg/L; this is probably due to the decrease in the resistance to lead ions uptake as the mass transfer driving force increased [44].

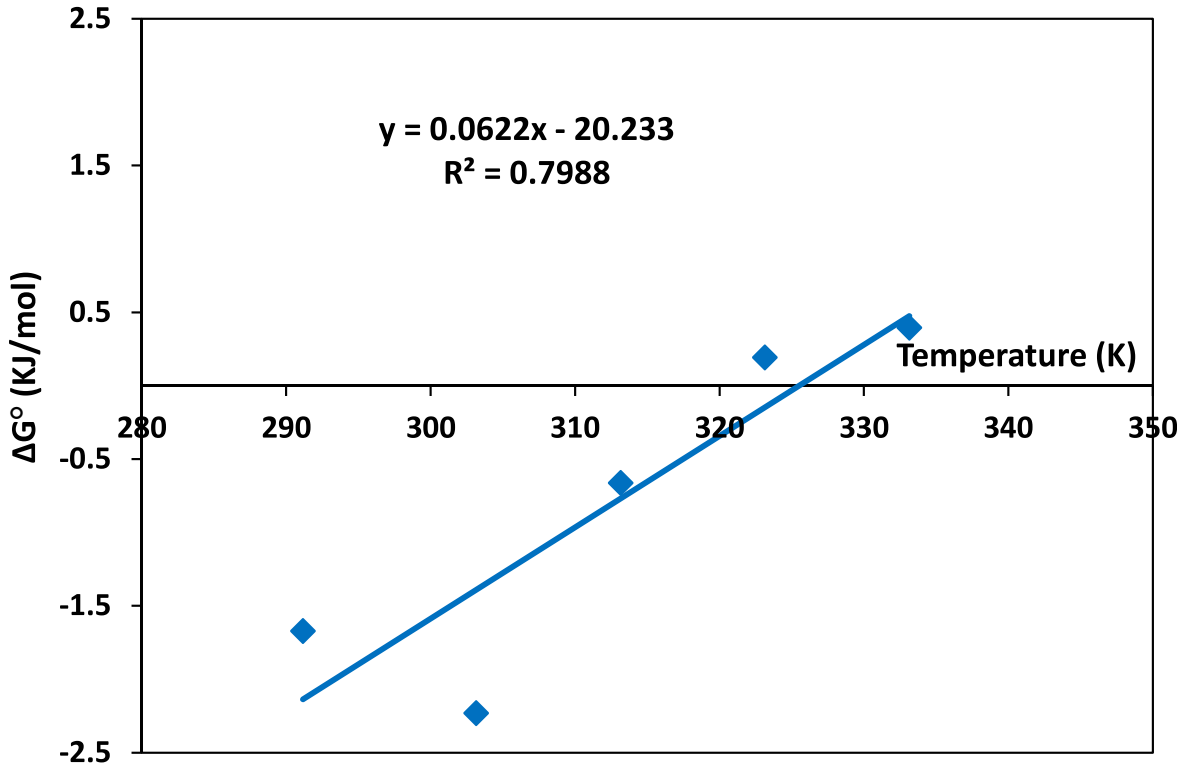

Fig. 12. Variation of Gibbs free energy change as function of temperature for Pb ions adsorption on CADS. [Pb2+]0 = 100 mg/L; adsorbent mass = 0.7 g; Vsoluion = 75 mL; stirring speed = 500 rpm/min; pH = 5.6 ± 0.2; T = 18 ± 2 °C.

Table 4
Thermodynamic parameters for the adsorption of Pb ions on carbonized and activated date stones "CADS". [Pb^{2+}] = 100 mg/L, volume of solution = 75 mL, mass of adsorbent = 0.7g, stirring speed = 500 rpm/min, pH = 5.6 ± 0.1.

lnK_d	Temperature(°C)	ΔG° (kJ/mol)	ΔS° (kJ/mol.K)	ΔH° (kJ/mol)
0.0492	18	−1.67	−0.062	−20.23
0.1307	30	−2.23		
0.2116	40	−0.66		
0.3571	50	0.19		
0.3580	60	0.39		

3.2. Adsorption of Pb ions in mixed solutions

The adsorption capacity of CADS towards Pb ions in mixed solutions; i.e. cobalt ions; has been investigated, see Fig. 6a. The initial concentration of Pb(II) varies 100, 200, 300, 400 and 500 mg/L ($4.83.10^{-4}$, $9.65.10^{-4}$, $14.48.10^{-4}$, $19.31.10^{-4}$ and $24.13.10^{-4}$ M) while the concentration of Co(II) is 3.5 the concentration of Pb(II). Herein, it is important to highlight that the chosen range of concentration is equivalent to that of Algerian industrial discharges. From Fig. 6a, it can be observed that an increase in initial metal concentration leads to a decrease in the adsorption efficiency. The impact is more pronounced at low concentrations, in particular at 100 mg/L wherein the adsorption rate of Pb ions drops significantly up to 32%. Since all metal ions are divalent, this decline in the adsorption can be attributed to the steric factor (the ionic radius of Pb2+ is larger compared to that of Co2+; 119 and 65 p.m. respectively), as consequence Co(II) can access to the active sites on the adsorbent surface more easily compared to Pb(II) thereby reducing the adsorption rate of Pb ions.

Some researchers have studied the simultaneous adsorption of Hg^{2+}, Pb^{2+} and Cu^{2+} from aqueous solution via Yarrowia lipolytica 70,562 living mass. They have recorded a decrease in lead ions uptake as the initial ions concentration increases. This decrease may be due to competition among Pb(II) ions with the other ions for limited number of accessible active sites because of their saturation [50].

In contrast, the amount of Pb ions increases as the initial concentration in the medium is increased; single and mixed solutions; because the ionic strength becomes more important which leads to a greater mass transfer.

FTIR spectral analysis of the adsorbent (Fig. 6b) undergoing adsorption of Pb(II) contained in single [$Pb(NO_3)_2$] and mixed [$Pb(NO_3)_2$/$Co(NO_3)_2{\cdot}6H_2O$] solutions, reveal that CADS has kept the same surface functional groups, as discussed previously in Fig. 3 (Red curve).

3.3. Comparison between the adsorption capacities of CADS and CAC

The carbonized and activated carbon made from date stones "CADS" has shown an efficiency as good as commercial coal throughout the experimental concentration range 100–700 mg/L (Fig. 7). It should be noted that, at lower concentration of 100 mg/L, the adsorption on CADS (R = 96.86%, X/m = 10.38 mg/g) is greater than that of CAC (R = 75.82%, X/m = 8.12 mg/g) and the adsorbed amount is enhanced as higher concentration. Indeed, date stones are a potential source for the production of a cost-effective activated carbon for the removal of heavy metals.

3.4. Adsorption of Pb ions assisted by ultrasound radiation

3.4.1. Effect of sonolysis time

The adsorption of Pb ions on CADS with and without ultrasonic radiation has been examined by varying the sonolysis time from 10 to 240 min, see Fig. 8a. As can be seen, an identical trend is observed for the adsorption curves, revealing a gradual increase as a function of time until reaching a stable state at 180 min. This equilibrium time is considered sufficient to achieve saturation, in agreement with the literature [30,51].

The hybrid technique using adsorption under ultrasound has proven to be more effective than in stirring batch mode. The removal efficiency of Pb(II) from feed solutions is found to increase up to 98.16% (X/m =

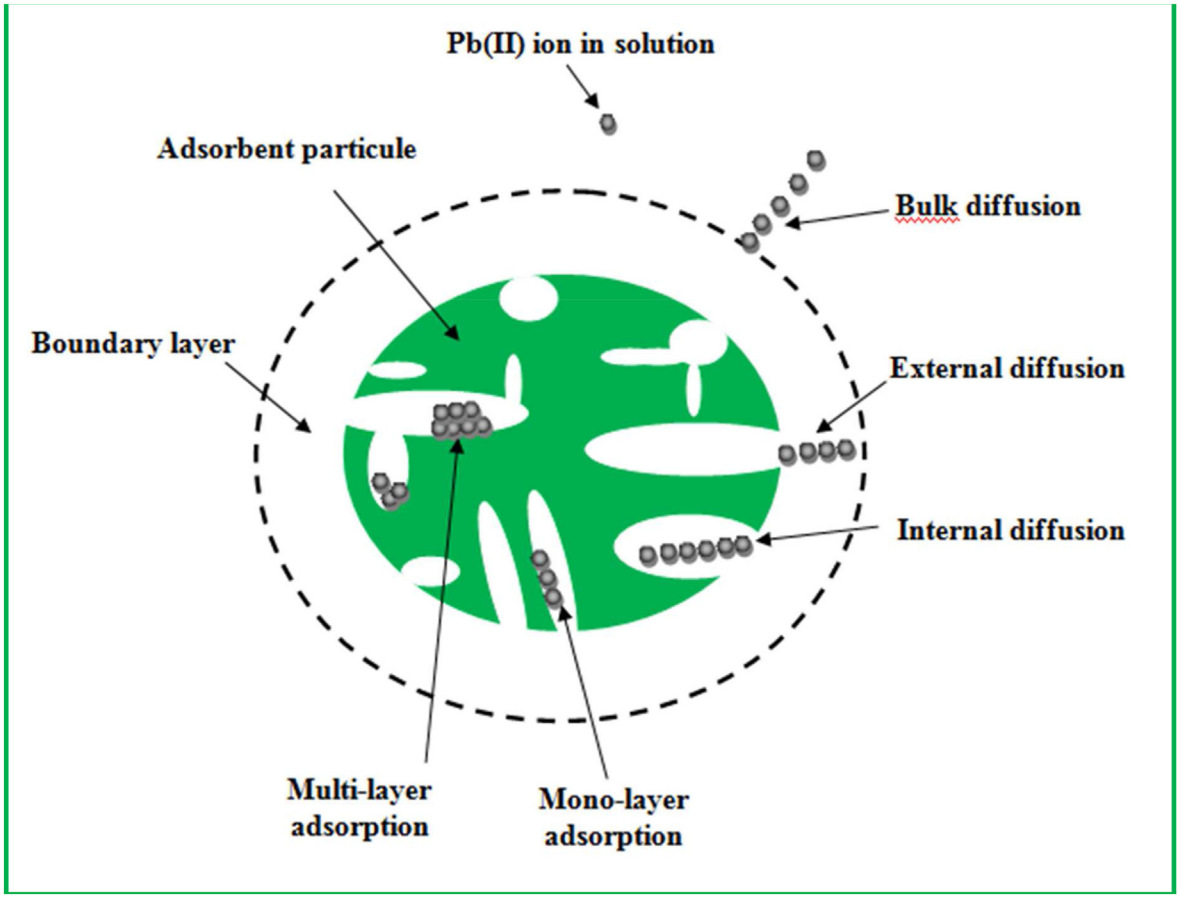

Fig. 13. Adsorption mechanism of Pb ions on CADS.

10.52 mg/g) under ultrasound instead of 94.9% (X/m = 10.17 mg/g) under magnetic stirring. Alipanahpour Dil et al. have shown that the simultaneous removal of lead ions and malachite green dye from aqueous solutions by adsorption on the copper oxide nanoparticle-loaded activated carbon assisted with ultrasound is strongly affected by the sonication time; hence the removal rate increases with increasing ultrasound irradiation time [52].

The utilization of sound waves enhances the adsorption of Pb ions due to the acoustic cavitation which increases mass transfer process at the surface and the pores within the adsorbent [30,53,54]. The diverse effects of cavitation process namely turbulence phenomenon and microstreaming cause a better mass transfer of solute from solution to the adsorbent surface. Other effects; i.e. micro-jets and shockwaves, may also cause the creation of supplementary adsorption sites on the adsorbent surface leading to much enhanced efficiency [35]. On the hand, the acoustic cavitation induces a rise in the medium temperature and pressure close to the adsorbent surface which can also affect its morphological appearance and create other active sites favoring further enhancement in the adsorption capacity [35,55,56].

3.4.2. Effect of temperature

The effect of temperature in the presence of ultrasound is studied by varying the medium temperature from 18 to 60 °C. The temperature was controlled by water circulating from a thermostatic bath through a copper cooling system. In the first step, the adsorption efficiency slightly increases when varying the temperature from 18 to 30 °C (Fig. 8b), this phenomenon can be ascribed to the increase in the diffusion rate of Pb ions with increasing temperature, following the decrease in the viscosity of solution [31]. Beyond 30 °C, the efficiency decreases from 98.77 to 92.70% after 180 min of ultrasound irradiation. Similar results have been reported in the literature, where the adsorption capacity of Pb ions drops with increasing temperature due to the tendency of these ions to escape from the adsorbent surface into the solution leading to a reduction in the thickness of boundary layer [45,57].

In this study, the effect of temperature is assisted by the utilization of ultrasound irradiation, which facilitates the formation of cavitation bubbles due to a decrease of the liquid tensile stress and viscosity [35]. Therefore, the collapse bubbles near the surface participate strongly in the dispersion of Pb ions and disrupt the adsorption phenomenon which can support the hypotheses reported previously in the literature [31,35].

Furthermore, the adsorption of Pb ions is found to be improved under ultrasound irradiation compared to conventional method over the entire studied temperature range. Sonication improve the adsorption of metal ions through the extreme conditions created by cavitation bubbles which provide a sufficient energy for better interaction with the active sites present at the adsorbent surface [31].

3.5. Modeling

3.5.1. Adsorption isotherms

Adsorption isotherms are expressed by the variation of the adsorbed solute amount q_e versus the equilibrium concentration C_e. The Freundlich (4) and Langmuir (5) equations are used in their linearized form:

$$\frac{X}{m} = K_F . C_e^{1/n} \tag{4}$$

$$\frac{X}{m} = a . b . \frac{C_e}{(1 + a . C_e)} \tag{5}$$

where KF and n are constants characteristic of the efficiency of a given

adsorbent towards a given solute, a is a thermodynamic equilibrium constant (L/mg), and b the maximum adsorption capacity (mg/g).

As shown in Fig. 9a, at Pb ions concentration 100 mg/L, the curve qe *vs.* C_e is compatible with the isotherm "L-type". It should be emphasized that the established modeling is related to the adsorption carried in stirred mode at various temperature (18, 30, 40, 50 and 60 °C).

Afterwards, the experimental data are fitted using Langmuir and Freundlich isotherms (Fig. 9b and c). For the Langmuir model, the adsorption sites are energetically equivalent whereas in the Freundlich model there is a coexistence of different energies distributed exponentially with the adsorption heat [26,38]. The quality of the isotherms fitting is assessed by the regression coefficient; then as can be seen in Table 1 the values of R^2 deduced from Langmuir model are generally closer to unity and slightly higher than those from Freundlich model (Table 1). Then both Langmuir and Freundlich models provided a reasonable fit to the isotherm data, which implies that the adsorption process is carried out in single and multi-layers simultaneously.

3.5.2. Adsorption kinetics

The adsorption kinetics of Pb ions by CADS is modeled using the first-order rate of Lagergren (Eq. (6)), the pseudo second-order rate (Eq. (7)) and the second order rate (Eq. (8)) [58,59]:

$$log(q_e - q_t) = logq_e - \frac{k_L}{2.3}.t \tag{6}$$

$$\frac{t}{q_t} = \frac{1}{(k'.q_e^2)} + \left(\frac{1}{q_e}\right).t \tag{7}$$

$$\frac{1}{(q_e - q_t)} = k.t + \frac{1}{q_e} \tag{8}$$

where k_L is the Lagergren rate constant of sorption (1/min), k' the pseudo-second-order rate constant of sorption (g/mg.min), k the rate constant (g/mg.min), q_e and q_t are the amounts of metal adsorbed (mg/g) at equilibrium and at a given time t, respectively.

In this context, the influence of temperature (18, 30, 40, 50 and 60 °C) on the adsorption kinetics of Pb ions in stirred mode has been studied. The results presented in Fig. 10a, indicate that the curves have the same shape characterized by a strong increase of the Pb(II) amount adsorbed by CADS during the first minutes of contact between the aqueous solution and the adsorbent, followed by a slow increase until reaching an equilibrium state at 180 min. Moreover, the rise of temperature from 18 to 30 °C provides a further increase in the amount of Pb(II) adsorbed at equilibrium; i.e. X/m increases from 10.17 mg/g to10.26 mg/g.

For an initial Pb(II) concentration of 100 mg/L, the constants values calculated from the slopes and intercepts of the linear plots log(q_e-q_t) *vs.* t, t/q_t *vs.* t, and 1/(q_e−q_t) *vs.* t (Fig. 10b–d) are summarized in Table 2. It can be noted that only the pseudo-second-order reaction rate model adequately describes the adsorption kinetics of Pb ions with a relatively high R^2 value of 0.999 (Fig. 9c) and a calculated values "$q_{e\ cal}$" very close to those obtained experimentally "$q_{e\ exp}$". This result is in good agreement with the literature; the elaborate kinetic studies indicate that the adsorption reaction of Pb ions follows a pseudo-second-order model [52, 60–63].

3.5.3. Diffusion process

Modeling the transfer phenomenon of a solute from a liquid phase to a solid phase, to express the external diffusion, is often given by Ref. [43]:

$$ln\frac{C_0 - C_e}{C_t - C_e} = k_{ex}.t \tag{9}$$

where C_t is the ions concentration at time t and k_{ext} is the constant of external diffusion. The plot ln[(C_0–C_e)/(C_t-C_e)] *vs.* t helps to assess whether the external diffusion step is decisive for the adsorption phenomenon.

From Fig. 11a, describing the modeling of adsorption at room temperature (18 ± 2 °C), it is clearly observed that the external diffusion of Pb(II) between the adsorbent particles is not a critical-step in the adsorption process because the experimental data is not well-fitted by this model (R^2 values are not high). The values of external diffusion constant k_{ex} and R^2 are given in Table 3 (figures not shown here).

According to Wu et al., the intraparticle diffusion kinetics expression is often presented by the simple equation [64]:

$$q_t = k_{in}.t^{1/2} + C \tag{10}$$

where q_t is the quantity adsorbed at a given time t, k_{in} is the internal diffusion constant and C is a constant related to the thickness of the boundary layer.

The modeling of the Pb(II) adsorption on CADS at ambient temperature (18 ± 2 °C) is illustrated in Fig. 11b. Indeed, the experimental data are aligned with a considerable regression coefficient (R^2 = 0.9879); indicating that the intraparticle diffusion process can be considered as limiting step in the adsorption process. In addition, the modeling results (k_{in} and R^2) of intraparticle diffusion kinetics for different temperatures are given in Table 3 (figures not shown here). It can be noticed that the R^2 values of the intraparticle diffusion kinetics are higher compared to that of external diffusion and close of the unity, which confirms that the intraparticle diffusion is a limiting-step controlling the transfer of Pb ions from solution towards CADS. Several studies carried out on the adsorption of heavy metals including Pb(II) on different materials showed that the pore diffusion contributed more to intraparticle diffusion than the surface diffusion [50,60–62,65].

3.5.4. Thermodynamic study

In thermodynamic studies, both energy and entropy factors must be considered in order to determine which process will occur spontaneously. The Gibbs free energy change (ΔG°) is the fundamental criterion; a process occurs spontaneously at a given temperature if ΔG° is a negative quantity. To estimate the effect of temperature on Pb(II) adsorption by CADS, the Gibb's free energy (ΔG^0), enthalpy change (ΔH^0) and entropy change (ΔS^0) have been determined by means of the following equations [66]:

$$\Delta G^0 = -R.T.lnK_d \tag{11}$$

$$\Delta G^0 = \Delta H^0 - T.\Delta S^0 \tag{12}$$

where $K_d = q_e/C_e$, T is the absolute solution temperature (K) and R is the universal gas constant. As shown in Fig. 12, the plot ΔG° *vs.* T is linear, where the values of ΔH° and ΔS° represent the slope and intercept, respectively and the calculated parameters are given in Table 4.

The negative values of ΔG^0 at temperatures of 18, 30 and 40 °C (i.e. −1.67 kJ/mol, −2.23 kJ/mol and −0.66 kJ/mol respectively) confirm the feasibility of the process and the spontaneous nature of adsorption, which is in good agreement with the literature for the adsorption of Pb ions by different adsorbents like clinoptilolite and magnetic nanoparticles as well as cyano containing organic-inorganic mesoporous silica framework (Fe_3O_4@TiO_2–CN) [67,68]. However, the positive values of ΔG^0 obtained at 50 and 60 °C (i.e. 0.19 kJ/mol and 0.39 kJ/mol respectively) indicate that the process becomes less spontaneous, similar phenomenon has been observed by Adebisi et al. for the adsorption of Pb and Zn ions from aqueous solution onto activated carbon prepared from palm oil mill effluent [69].

The negative value of ΔH^0 (−20.23 kJ/mol) confirms the exothermic character of Pb(II) adsorption, and since the value found was low (<40 kJ/mol) the adsorption is considered physical in nature which implies weak forces of attraction at the adsorbent/solution interface wherein the main forces involved are the electrostatic interaction, van der Waal

forces, π-π interaction, hydrogen bond, etc [6].

Likewise, the negative value of ΔS^0 (−0.062 kJ/mol) corresponds to a decrease in the randomness at the interface adsorbent/solution during the adsorption of metal ions; which signifies that the distribution order of lead ions on the adsorbent is important compared to that in the solution [70].

From the modeling study, the adsorption of lead ions on CADS over time can consist of four stages (Fig. 13): (1) transfer of Pb(II) from solution to the boundary layer i.e. the surface film surrounding the adsorbent particles (bulk diffusion); (2) transfer of Pb(II) through the boundary layer to the outside of the adsorbent particles (external diffusion); (3) transfer of Pb(II) within the adsorbent particles to the adsorption sites i.e. the limiting step (internal diffusion); and (4) physical adsorption of lead ions by the functional groups existing on the surface of CADS such as –OH, C–O, C═O and C–H; this is the exothermic step.

4. Conclusion

A low-cost process was adopted to transform date stones biowaste into cost-effective heavy metal ions adsorbent through simultaneous carbonization and activation processes. The optimization of operational parameters allows an excellent level uptake of lead ions on CADS surface (R = 97.43%). The adsorption isotherms of Pb ions on CADS are of "L type" and are satisfactory described by the Langmuir and Freundlich models. The kinetics study showed that the process follows pseudo second–order kinetics and controlled by the internal diffusion. The thermodynamic study pointed out that the system was spontaneous and exothermic. Throughout the studied concentration range, CADS exhibits better adsorption efficiency for lead ions (96.86%) compared to that of CAC (75.82%).

The adsorption of Pb ions on CADS under ultrasound irradiation proved an enhancement in the adsorption efficiency while an increase in medium temperature induced a negative effect. The adsorption of Pb ions was also affected by the presence of Co ions in the solution (a drop of 32%).

This study highlighted the importance of transforming biowaste, in this case date stones, into inexpensive adsorbents with enhanced characteristics as potential candidates for the removal of heavy metals as well as other organic pollutants from wastewaters.

Data availability

All methods and materials used in this study are well exposed in this article. For any other necessary information the author is ready to provide it upon request.

Declaration of competing interest

The authors declare no conflicts of interest.

Acknowledgments

The authors acknowledge the research grant provided by the Algerian Ministry of Higher Education and Scientific Research (project A16N01UN410120180002).

References

[1] Hussain A, Priyadarshi M, Dubey S. Experimental study on accumulation of heavy metals in vegetables irrigated with treated wastewater. Appl. Water Sci. 2019; 122(9):1–11.
[2] Arbabi M, Hemati S, Amiri M. Removal of lead ions from industrial wastewater: a review of removal methods. Int. J. Epidemiol. Res. 2015;2(2):105–9.
[3] Bouranene S, Fievet P, Szymczyk A, Samar MEH, Vidonne A. Influence of operating conditions on the rejection of cobalt and lead ions in aqueous solutions by a nanofiltration polyamide membrane. J. Membr. Sci. 2008;325:150–7.
[4] Sharma A, Sharma A, Arya RK. Removal of mercury (II) from aqueous solution: a review of recent work. Separ. Sci. Technol. 2015;50(9):1310–20.
[5] Fronczak M, Pyrzyńska K, Bhattarai A, Pietrowski P, Bystrzejewski M. Improved adsorption performance of activated carbon covalently functionalised with sulphur-containing ligands in the removal of cadmium from aqueous solutions. Int. J. Environ. Sci. Technol. 2019;16:7921–32.
[6] Wang L, Shi C, Wang L, Pan L, Zhang X, Zou J. Rational design, synthesis, adsorption principles and applications of metal oxide adsorbents: a review. Nanoscale 2020;12(8):4790–815.
[7] Das PN, Jithesh K, Raj KG. Recent developments in the adsorptive removal of heavy metal ions using metal-organic frameworks and graphene-based adsorbents. J. Indian Chem. Soc. 2021;98(11):100188.
[8] Wang H, Zhang Q, Qiu M, Hu B. Synthesis and application of perovskite-based photocatalysts in environmental remediation: a review. J. Mol. Liq. 2021;334: 116029.
[9] Liu F, Hua S, Wang C, Qiu M, Jin L, Hu B. Adsorption and reduction of Cr(VI) from aqueous solution using cost-effective caffeic acid functionalized corn starch. Chemosphere 2021;279:130539.
[10] Gupta SS, Bhattacharyya KG. Interaction of metal ions with clays: a case study with Pb(II). Appl. Clay Sci. 2005;30:199–208.
[11] Gupta SS, Bhattacharyya KG. Immobilization of Pb(II), Cd(II) and Ni(II) ions on kaolinite and montmorillonite surfaces from aqueous solutions. J. Environ. Manag. 2008;87:46–58.
[12] Kakaei S, Khameneh ES, Hosseini MH, Moharreri MM. A modified ionic liquid clay to remove heavy metals from water: investigating its catalytic activity. Int. J. Environ. Sci. Technol. 2020;17:2043–58.
[13] Huang Z, Wu P, Gong B, Dai Y, Chiang PC, Lai X, Yu G. Efficient removal of Co^{2+} from aqueous solution by 3-Aminopropyltriethoxysilane functionalized montmorillonite with Enhanced adsorption capacity. PLoS One 2016;11(7): e0159802.
[14] Basu A, Mustafiz S, Islam MR, Bjorndalen N, Rahaman MS, Chaalal O. A comprehensive approach for modelling sorption of lead and cobalt ions through fish scales as an adsorbent. Chem. Eng. Commun. 2006;193:580–605.
[15] Enkhzaya S, Shiomori K, Oyuntsetseg B. Removal of heavy metals from aqueous solution by adsorption using Livestock Biomass of Mongolia. J. Environ. Sci. Technol. 2017;10(3):107–19.
[16] Dawood S, KantiSen T, Phan C. Synthesis and characterization of slow pyrolysis pine cone bio-char in the removal of organic and inorganic pollutants from aqueous solution by adsorption: kinetic, equilibrium, mechanism and thermodynamic. Bioresour. Technol. 2017;246:76–81.
[17] Ali Alatabe MJ, ObaidKariem N. Thorns, a novel natural plants for adsorption of Lead (II) ions from wastewater equilibrium, isotherm, kinetics and thermodynamics. Eurasian J. Anal. Chem. 2019;14(2):163–74.
[18] Ali Alatabe MJ. A novel approach for adsorption of Lead (II) ions from wastewater using cane papyrus. J. Petrol. Res. Stud. 2018;18:29–42.
[19] OuYang XK, Yang LP, Wen ZS. Adsorption of Pb(II) from solution using peanut shell as biosorbent in the presence of amino acid and sodium chloride. Bioresources 2014;9(2):2446–58.
[20] Tseveendorj E, Enkhdul T, Lin S, Dorj D, Oyungerel Sh, Soyol-Erdene TO. Biosorption of lead (II) from an aqueous solution using biosorbents prepared from water plants. Mong. J. Chem. 2017;18(44):52–61.
[21] Krishnamoorthy R, Govindan B, Banat F, Sagadevan V, Purushothaman M, Show PL. Date pits activated carbon for divalent lead ions removal. J. Biosci. Bioeng. 2019; 128(1):88–97.
[22] Chaouch N, Ouahrani MR, Laouini SE. Adsorption of Lead (II) from aqueous solutions onto activated carbon prepared from Algerian dates stones of Phoenix dactylifera: L (Ghars variety) by H_3PO_4 activation. Orient. J. Chem. 2014;30(3): 1317–22.
[23] Boudrahem F, Aissani-Benissad F, Audonnet F, Vial C. Effects of acid-basic treatments of date stones on lead (II) adsorption. Separ. Sci. Technol. 2019;54(11): 1749–63.
[24] Mahdi Z, Yu QJ, El Hanandeh A. Removal of lead(II) from aqueous solution using date seed-derived biochar: batch and column studies. Appl. Water Sci. 2018;8(181): 1–13.
[25] Shafiq M, Alazba AA, Amin MT. Removal of heavy metals from wastewater using date palm as a biosorbent: a comparative review. Sains Malays. 2018;47(1):35–49.
[26] Aldawsari A, Khan MA, Hameed BH, Alqadami AA, Siddiqui MR, Alothman ZA, Hadj Ahmed AYB. Mercerized mesoporous date pit activated carbon-A novel adsorbent to sequester potentially toxic divalent heavy metals from water. PLoS One 2017;12(9):1–17.
[27] Al-Saidi HM. The fast recovery of gold(III) ions from aqueous solutions using raw date pits: kinetic, thermodynamic and equilibrium studies. J. Saudi Chem. Soc. 2016;20:615–24.
[28] Hamdaoui O. Intensification of the sorption of Rhodamine B from aqueous phase by loquat seeds using ultrasound. Desalination 2011;271:279–86.
[29] Hamdaoui O, Chiha M, Naffrechoux E. Ultrasound-assisted removal of malachite green from aqueous solution by dead pine needles. Ultrason. Sonochem. 2008;15: 799–807.
[30] Bdaiwi Ahmed S, Stoica-Guzun A, Kamar FH, Dobre T, Gudovan D, Busuioc C, Jipa IM. Ultrasound enhanced removal of lead from wastewater by hazelnut shell: an experimental design methodology. Int. J. Environ. Sci. Technol. 2019;16(4): 1249–60.
[31] Hamdaoui O. Removal of cadmium from aqueous medium under ultrasound assistance using olive leaves as sorbent. Chem. Eng. Process 2009;48:1157–66.
[32] Asfaram A, Ghaedi M, Hajati S, Goudarzi A, Bazrafshan AA. Simultaneous ultrasound-assisted ternary adsorption of dyes onto copper-doped zinc sulfide nanoparticles loaded on activated carbon: optimization by response surface methodology. Spectrochim. Acta Mol. Biomol. Spectrosc. 2015;145:203–12.

[33] Ramutshatsha-Makhwedzh D, Ngila JC, Ndungu PG, Nomngongo PN. Ultrasound assisted adsorptive removal of Cr, Cu, Al, Ba, Zn, Ni, Mn, Co and Ti from seawater using Fe_2O_3-SiO_2-PAN nanocomposite: equilibrium kinetics. J. Mar. Sci. Eng. 2019; 7(5):1–16.
[34] Iconaru SL, Motelica-Heino M, Guegan R, Predoi MV, Prodan AM, Predoi D. Removal of zinc ions using hydroxyapatite and study of ultrasound behavior of aqueous media. Materials 2018;11(8):1–16.
[35] Pugazhenthiran N, Anandan S, Ashokkumar M. Removal of heavy metal from wastewater. In: Book: Handbook of Ultrasonics and Sonochemistry; 2016. p. 813–39.
[36] Roosta M, Ghaedi M, Daneshfar A, Sahraei R. Experimental design based response surface methodology optimization of ultrasonic assisted adsorption of safaranin O by tin sulfide nanoparticle loaded on activated carbon. Spectrochim. Acta Mol. Biomol. Spectrosc. 2014;122:223–31.
[37] Hazourli S, Ziati M, Hazourli A, Cherifi M. Valorisation d'un résidu naturel lignocellulosique en charbon actif -exemple des noyaux de dattes. Revue des Energies Renouvelables ICRESD-7 Tlemcen 2007:187–92.
[38] Sekirifa ML, Hadj-Mahammed M. Etude comparative de la capacité adsorbante d'un charbon actif issue de noyau de dattes et un charbon actif commercial. Sci. Technol., B 2005;23:55–9.
[39] Bestani B, Benderdouche N, Benstaali B, Belhakem M, Addou A. Methylene blue and iodine adsorption onto an activated desert plant. Bioresour. Technol. 2008;99: 8441–4.
[40] Swiatkowski A, Pakula M, Biniak S, Walczyk M. Influence of the surface chemistry of modified activated carbon on its electrochemical behaviour in the presence of lead(II) ions. Carbon 2004;42:3057–69.
[41] Li Y, Du Q, Wang X, Zhang P, Wang D, Wang Z, Xia Y. Removal of lead from aqueous solution by activated carbon prepared from Enteromorphaprolifera by zinc chloride activation. J. Hazard Mater. 2010;183:583–9.
[42] Benaïssa H, Elouchdi MA. Biosorption of copper (II) ions from synthetic aqueous solutions by drying bed activated sludge. J. Hazard Mater. 2011;194:69–78.
[43] Belaid KD, Kacha S. Study of the kinetics and thermodynamics of the adsorption of a basic dye on sawdust. J. Water Sci. 2011;24(2):131–44.
[44] Guechi EK, Hamdaoui O. Sorption of malachite green from aqueous solution by potato peel: kinetics and equilibrium modeling using non-linear analysis method. Arab. J. Chem. 2016;9:416–24.
[45] Jnr MH, Spiff AI. Effects of temperature on the sorption of Pb^{2+} and Cd^{2+} from aqueous solution by Caladium bicolor (Wild Cocoyam) biomass. Electron. J. Biotechnol. 2005;8(2):162–9.
[46] Leon y Leon CA, Radovic LR. Interfacial chemistry and electrochemistry of carbon surfaces. In: Thrower PA. Chem. Phys. Carbon., vol. 24; 1994. p. 213–310.
[47] Mohammadi SZ, Karimi MA, Afzali D, Mansouri F. Removal of Pb (II) from aqueous solutions using activated carbon from Sea-buckthorn stones by chemical activation. Desalination 2010;262:86–93.
[48] Boujelben N, Bouzid J, Elouear Z. Removal of lead (II) ions from aqueous solutions using manganese oxide-coated adsorbents: characterization and kinetic study. Adsorpt. Sci. Technol. 2009;27:177–91.
[49] Alghamdi AA, Al-Odayni AB, Saeed WS, Al-Kahtani A, Alharthi FA, Aouak T. Efficient adsorption of Lead (II) from aqueous phase solutions using Polypyrrole-Based activated carbon. Materials 2019;12(12):1–16.
[50] Alipanahpour Dil E, Ghaedi M, Ghezelbash GR, Asfaram A, Mihir Purkait MK. Highly efficient simultaneous biosorption of Hg^{2+}, Pb^{2+} and Cu^{2+} by Live yeast Yarrowia lipolytica 70562 following response surface methodology optimization: kinetic and isotherm study. J. Ind. Eng. Chem. 2017;48:162–72.
[51] Pehlivan E, Altun T, Cetin S, Bhanger MI. Lead sorption by waste biomass of hazelnut and almond shell. J. Hazard Mater. 2009;167:1203–8.
[52] Alipanahpour Dil E, Ghaedi M, Asfaram A, Hajati S, Mehrabi F, Goudarzi A. Preparation of nanomaterials for the ultrasound-enhanced removal of Pb^{2+} ions and malachite green dye: chemometric optimization and modeling. Ultrason. Sonochem. 2017;34:677–91.
[53] Dil EA, Ghaedi M, Asfaram A, Hajati S, Mehrabi F, Goudarzi A. Preparation of nanomaterials for the ultrasound-enhanced removal of Pb^{2+} ions and malachite green dye: chemometric optimization and modeling. Ultrason. Sonochem. 2017;34: 677–91.
[54] Renu, Agarwal M, Singh K. Heavy metal removal from wastewater using various adsorbents: a review. J. Water Reuse Desalin. 2017;7(4):387–419.
[55] de La Rochebrochard S, Naffrechoux E, Drogui P, Mercier G, Blais JF. Low frequency ultrasound-assisted leaching of sewage sludge for toxic metal removal, dewatering and fertilizing properties preservation. Ultrason. Sonochem. 2013;20: 109–17.
[56] Zhang P, Ma Y, Xie FC. Impacts of ultrasound on selective leaching recovery of heavy metals from metal-containing waste sludge. J. Mater. Cycles Waste Manag. 2013;15:530–8.
[57] Aksu Z, Kutsal TA. A bioseparation process for removing Pb(II) ions from wastewater by using C. vulgaris. J. Chem. Technol. Biotechnol. 1991;52(1):108–18.
[58] Lagergren S. About the theory of so-called adsorption of soluble substances. K. Sven. Vetenskapsakad. Handl. 1898;24(4):1–39.
[59] Ho YS, McKay G. The kinetics of sorption of divalent metal ions onto sphagnum moss peat. Water Res. 2000;34(3):735–42.
[60] Huda BN, Wahyuni ET, Mudasir M. Eco-friendly immobilization of dithizone on coal bottom ash for the adsorption of lead(II) ion from water. Results Eng. 2021;10: 100221.
[61] Abou-Zeid RE, Kamal KH, Abd El-Aziz ME, Morsi SM, Kamel S. Grafted Tempo-oxidized cellulose nanofiber embedded with modified, magnetite for effective adsorption of lead ions. Int. J. Biol. Macromol. 2021;167:1091–101.
[62] Claros M, Kuta J, El-Dahshan O, Michalička J, Jimenez YP, Vallejos S. Hydrothermally synthesized MnO_2 nanowires and their application in Lead (II) and Copper (II) batch adsorption. J. Mol. Liq. 2021;325:115203.
[63] Sharifpour E, Khafri HZ, Ghaedib M, Asfaramb A, Jannesar R. Isotherms and kinetic study of ultrasound-assisted adsorption of malachite green and Pb^{2+} ions from aqueous samples by copper sulfide nanorods loaded on activated carbon: experimental design optimization. Ultrason. Sonochem. 2018;40:373–82.
[64] Wu FC, Tseng RL, Juang RS. Initial behavior of intraparticle diffusion model used in the description of adsorption kinetics. Chem. Eng. J. 2009;153:1–8.
[65] Maia MT, Sena DN, Calais GB, Luna FMT, Beppuc MM, Vieira RS. Effects of histidine modification of chitosan microparticles on metal ion adsorption. React. Funct. Polym. 2020;154:104694.
[66] Nandi BK, Goswami A, Purkait MK. Adsorption characteristics of brilliant green dye on kaolin. J. Hazard Mater. 2009;161:387–95.
[67] Pandey S, Fosso-Kankeu E, Spiro MJ, Waanders F, Kumar N, Ray SS, Kim J, Kang M. Equilibrium, kinetic, and thermodynamic studies of lead ion adsorption from mine wastewater onto MoS_2-clinoptilolite composite. Mater. Today Chem. 2020;18: 100376.
[68] Mousavi SV, Bozorgian A, Mokhtari N, AliGabris M, Nodeh HR, Wan Ibrahim WA. A novel cyanopropylsilane-functionalized titanium oxide magnetic nanoparticle for the adsorption of nickel and lead ions from industrial wastewater: equilibrium, kinetic and thermodynamic studies. Microchem. J. 2019;145:914–20.
[69] Adebisi GA, Chowdhury ZZ, Alaba PA. Equilibrium, kinetic, and thermodynamic studies of lead ion and zinc ion adsorption from aqueous solution onto activated carbon prepared from palm oil mill effluent. J. Clean. Prod. 2017;148:958–68.
[70] Olgun A, Atar N. Equilibrium, thermodynamic and kinetic studies for the adsorption of lead (II) and nickel (II) onto clay mixture containing boron impurity. J. Ind. Eng. Chem. 2012;18:1751–7.